SYNTHESIS OF DOXORUBICIN-ALBUMIN CONJUGATES VIA COBALT COORDINATION CHEMISTRY: THE EFFECT OF REACTION CONDITIONS ON OVERALL PROTEIN STABILITY

A THESIS

SUBMITTED IN A PARTIAL FULFILLMENT OF THE REQUIREMENTS

FOR THE DEGREE OF MASTER OF SCIENCE

IN THE GRADUATE SCHOOL OF THE

TEXAS WOMAN'S UNIVERSITY

DEPARTMENT OF CHEMISTRY AND BIOCHEMISTRY

COLLEGE OF ARTS AND SCIENCE

BY

ASHIK PATEL, B.S.

DENTON, TEXAS

MAY 2022

Copyright © 2022 by Ashik Patel

DEDICATION

I dedicate my thesis to my parents and friends. The master's degree for me would not be possible without you. I would like to thank my cousin for all his support throughout my educational journey in the United States. Thank you for everything you do. I would never forget the sacrifice you made for me to achieve my master's degree

ACKNOWLEDGEMENTS

I would like to take an opportunity to thank my mentor Dr. Robby Petros. I am grateful for everything I have learned from you as both an undergraduate student and as a graduate student. I appreciate you believing in me and for allowing me to join your research group. I look forward to utilizing the skills and knowledge you help instill in me in a positive way.

I would like to thank Dr. Robby Petros and Dr. Manal Omary for always being there for me, and for being very responsive whenever I needed anything relating to the university.

I would also like to thank my prospectus and thesis committee Dr. Richard Sheardy, Dr. Robby Petros and Dr. Salazar. I really appreciate you all for considering my work and dedication as a graduate student and allowing me to present my thesis to you.

ABSTRACT

SYNTHESIS OF DOXORUBICIN-ALBUMIN CONJUGATES VIA COBALT COORDINATION CHEMISTRY: THE EFFECT OF REACTION CONDITIONS ON OVERALL PROTEIN STABILITY

MAY 2022

The applications of nanotechnology in designing better treatments shows great promise in lessening the burden of chemotherapy while increasing therapeutic effect. Protein-drug conjugates are a rapidly expanding family of therapeutics that hold potential for ameliorating off-target toxic effects observed in chemotherapy. In this context, human serum albumin could act as a nanoscale delivery vector to alter the biodistribution of attached therapeutics.

This research explored the use of cobalt coordination chemistry in the synthesis of Dox-albumin conjugates. Doxorubicin was chosen because it contains a primary amine that could be crosslinked to protein using cobalt coordination chemistry. The effect of pH and reaction time on the synthesis of conjugates was investigated. Samples were characterized by High Performance Liquid Chromatography, Dynamic Light Scattering, and Differential Scanning Calorimetry. Optimized reaction conditions for synthesizing conjugates with varying numbers of dox molecules per protein was a major focus of the research.

TABLE OF CONTENTS

LIST OF TABLES

LIST OF FIGURES

CHAPTER I

INTRODUCTION

Introduction

Cancer has been one of the deadliest diseases to ever exist in the world "standing second to heart related disorders (cardiovascular diseases)" in terms of sources of death.[1] The word cancer is derived from the Greek word karkinos. The great Greek physician Hippocrates was first known to use this word to express the formation of tumors with ulcers (which was named carcinos, a non-cancer tumor) and the formation of tumors without ulcers (which were named carcinoma- a cancerous tumor).[2,3] The spread of cancer in a human body is a fingerlike appearance resembling the shape of a crab.

The simple definition of cancer is a disease in which the growth of normal cells at a particular region of body becomes dysregulated. There are various types of cancer depending on the region or a part of the body. The phenomenon of normal cells growing at a faster rate and becoming abnormal instead of going under apoptosis remains the hallmark of all types of cancers. In many types of cancer, cancerous cells migrate to other different parts of the body/organs through the lymphatic system, but it does not mean that it is cancerous in the part of the body where those cancerous cells accumulated. It is still the same cancer from where those cells originated and is a process known as metastasis.[4]

Cancer can be classified into two major types in terms of its occurrence:

1. Acquired cancers: In this type of cancer the cancerous cells are produced from the normal cells by mutation. This happens when DNA of normal cells is damaged by carcinogens. These carcinogens can be either a chemical substance (various organic solvents like benzene), light (like

UV radiations), or a biological substance (virus like hepatis B or hepatis C). Our body is capable of healing most of the damaged DNA, but some damages are non-repairable which leads to cancer.

2. Innate cancers: These cancers are inherited by an individual from their parents. The damaged part of DNA of a parent can be transferred over to the progeny and the child would either have (or not have) that type of cancer.[4]

The World Health Organization reported approximately 9.6 million people lost their lives due to cancer worldwide in 2018.[1] There was also an occurrence of about 3 million cases of cancer among children from age of 0-19 years.[1] The modernized treatment for cancer includes immunotherapy, hormonal therapy, chemotherapy, radiation therapy, and surgical procedures. Of these, the most common treatments are surgical procedures, radiation therapy, and chemotherapy. Surgical procedures focus on physically removing the tumor or the organ. The location of the tumor or the damaged organs are first traced by using magnetic resonance imaging (MRI) or sonography (ultrasound). Surgical procedures are then done with the camera attached to the surgical tools. Liquid nitrogen, with its very low temperature, has been used more recently to kill cancerous cells in a tumor. Laser surgeries are also highly utilized by surgeons and can be used to cut the tumors from the body without an incision.[3] The main drawback for surgical procedures is the likelihood that some small number of cancer cells will remain leading to regrowth after the tumor removal. Chemotherapy and radiation therapy go hand in hand whenever treating a patient with cancer. Traditional chemotherapeutics continue to induce toxic effects in healthy, non-cancerous cells.[5] The main drawbacks of chemotherapy are the very low bioavailability of the drugs to the cancerous cells. The chemotherapeutic drugs tend to accumulate in various vital organs of the body like the kidney, heart, liver, and others, where the drug starts showing its toxicity. Many anti-cancer drugs have a low rate of clearance from the body. Too often, the body

builds resistance towards certain chemotherapeutic drugs.[6] One alternative to avoid resistance is administering drugs in combinations of two or more. Better targeting of such therapies to only the diseased cells remain an ambitious goal. The use of nanotechnology in designing better treatments holds great promise in lessening the burden of chemotherapy on patients while simultaneously producing an increased therapeutic effect.[7] Nanotechnology also has opened the doors for research and development of a wide variety of nanomaterials. Nanomaterials have demonstrated effectiveness in minimizing side effects mentioned above for chemotherapeutic drugs.[8] Physical properties of nanomaterials such as size, shape, and texture play a key role in making an effective anti-cancer drug. Different sizes of nanomaterials have unique importance which can be used for a particular application only. Nanoparticle size can range from one nanometer to 1000 nanometers depending upon its applications. Monodisperse nanoparticles can be used as an anti-cancer drug, and the uniform sized nanoparticles are also an essential requirement for targeted drug delivery. The synthesis of nanoparticles specifically for encapsulating chemotherapeutic drugs should be of optimal size, meaning it should not be too small (not smaller than 10 nm) or too large (not larger than 200 nm). The drug loaded with the nanoparticles smaller than ≈10 nm can extravasate circulatory blood vessels quickly with no or less therapeutic action and can be easily removed from circulation through the kidneys. Nanoparticles larger than ~200 nm in size can be quickly removed by the reticuloendothelial system (RES), which consists of Kupfer cells in the spleen or liver.

The first polymer-drug conjugate synthesized in the 1950s was mescaline attached to polyvinylpyrrolidine. However, the conjugate did not release mescaline in vivo. By adding an enzymatically cleavable peptide spacer between mescaline and the polymer, extended release of Mescaline was observed.[9,10] Another major nanotechnological approach to targeted drug delivery emerged in the 1960s with the use of liposomes to encapsulate therapeutics, which also displayed

extended-release patterns in vivo.[11,12] Protein-based nanoparticles were first reported in the 1970s.[13] The first protein-based nanoparticle loaded with Paclitaxel (Abraxane) was approved for use by the FDA in 2005.[14]

Doxorubicin (A broad spectrum Anti-Cancer drug)

Doxorubicin belongs to the anthracycline group of pharmaceuticals. It is a 14-hydroxylated form of Daunorubicin (see Figure 1). Doxorubicin is broad spectrum, anti-neoplastic drug, which can be used for a variety of cancers like ovarian, bladder, breast, and lung cancer.[15,16] Doxorubicin is a red-colored crystalline solid. It was first discovered from castle soil in Italy in the 1950s. During the same time, French scientists also discovered the same drug. The name Daunorubicin was given to the drug after "Dauno," which is the name of tribal community, and "rubis," which means red. Doxorubicin can be extracted from the bacteria *streptomyces pencetius var caesium.*[17]

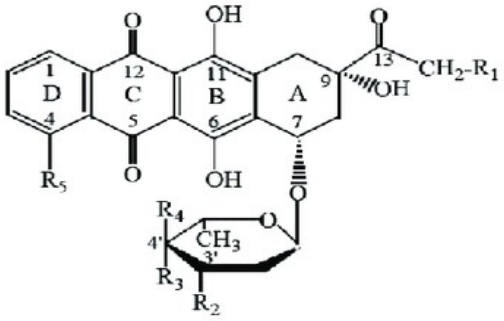

	R_1	R_2	R_3	R_4	R_5
daunorubicin	H	NH_2	OH	H	OCH_3
idarubicin	H	NH_2	OH	H	H
doxorubicin	OH	NH_2	OH	H	OCH_3
epidoxorubucin	OH	NH_2	H	OH	OCH_3
pirarubicin	OH	NH_2	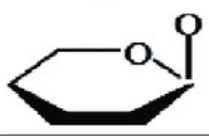	H	OCH_3

Figure 1. Common anthracycline derivatives used as of pharmaceuticals.[18]

Doxorubicin exerts its therapeutic effect in human cancer cells by inhibiting the enzyme topoisomerase II, which plays an important role in DNA replication. Topoisomerase II helps DNA

to remove unwanted supercoils during replication and DNA transcription. It also maintains a proper link between two DNA strands via phosphodiester bond. The binding of Doxorubicin to DNA induces structural changes in a DNA molecule that blocks the formation of the phosphodiester bond. This prevents further DNA replication and protein synthesis.[19] One of the drawbacks of using Doxorubicin is that it produces a large amount of free oxygen radicals, which contributes to the cytotoxicity of the drug. These free radicals can damage the cell membranes by withdrawing electrons from the lipid bilayer through oxidative degradation. Such damage of cell membranes can lead to cutaneous or cardiac (or both) vasculature consequences. The free radicals can also alter the process of myocytes by reacting with iron which can lead to cardio toxicity, which is one of the major side effects of Doxorubicin.

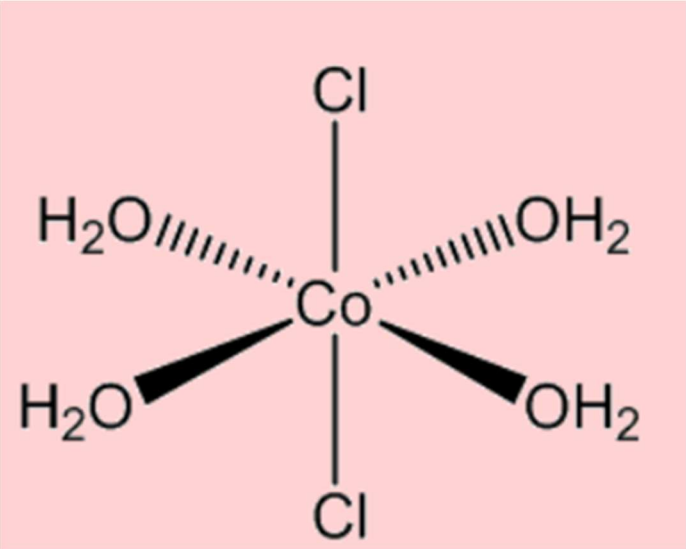

Figure 2. Chemical structure of cobalt chloride hexa aqua complex.[20]

Targeted Drug Delivery and A Fusion of Protein and Drug

To obtain a maximum degree of drug delivery at the cellular level, the drug should cross many biological barriers at the system level, at an organ level, and at the cellular level. The barriers are different depending on the route of administration. The bio availability of the drug to the targeted site through any route of drug administration heavily depends on the characteristics of

nanoparticles. For example, for oral administration, the stability of the drug-carrier conjugate must remain stable in a highly acidic medium (stomach) or highly basic medium (intestine-extended release). The nature of the prodrug should remain constricted within the circulatory system, minimizing the level of toxicity in the body and maximizing the bio availability of the drug at the targeted site. Doxorubicin-albumin prodrug conjugate is a large molecule and has a capability of being constricted with the circulatory system and not being dispersed or widely distributed all over the body. The experiment also emphasizes a drug-protein conjugate that uses the phenomena of enhanced permeability and retention effect (EPR effect). The EPR is a result of immature vasculature in tumors that are "leaky." This vasculature allows delivery vectors of up to 300 nm in size to exit circulation. Albumin has also been shown to accumulate in greater amounts near tumors and is a significant source of nutrients to the cancerous cells.[21]

For our research, human serum albumin (HSA) was used as a drug carrier. HSA is the most abundant serum protein in the body.[22] HSA is a well-known transporter of various nutrients and many hydrophobic molecules via non-covalent binding sites present in its structure.[23] HSA is a monomeric protein which consists of 585 amino acids and has a molecular mass of 66.5 KDa. HSA has three domains which make a heart shape. All three domains are made up of two or more subdomains. HSA also contains 17 disulfide bridges along with a sulfhydryl group in its free form on a cysteine residue.[24] This research mainly focuses on the three parts of a drug-protein conjugate which are: Doxorubicin (drug), HSA (protein), and cobalt (cross-linker). HSA itself can transport the drug to the targeted site,[25] and the crosslinking between biopolymer and drug can be accomplished via cobalt coordination chemistry.

Cobalt chloride in its hexa aqua form ($COCl_2.6H_2O$) was utilized as the source of cobalt (see Figure 2). Cobalt is a required trace element for a human body and is utilized by variety of

metalloenzymes. Previous studies have been conducted using cobalt as a bio conjugation technique; however, the method is dependent on the use of poorly labile cobalt in the 3+ -oxidation state.[25] Our group attempted utilizing this strategy as a generic amine cross linker and was not successful. To overcome this problem, my research team came up with a better technique of utilizing a more labile form of cobalt in the 2+ oxidation state. Cobalt (2+) chloride undergoes rapid ligand exchange and can be made inert (Co^{3+}) by the addition of hydrogen peroxide. This made the cross-linking bonds very stable. One more beneficial aspect of utilizing cobalt coordination chemistry is it allows for the conjugation of up to six amine-containing molecules. This is in stark contrast to other bio conjugation techniques that are typically limited to two amine-containing molecules.[22] The overall reaction used the only lone pair of electrons, present on the nitrogen atom of the amine group by forming a dative linkage between the nitrogen and cobalt. This reaction was used to crosslink between doxorubicin, which contains a primary amine (see Figure 3), and the lysine residues. Once cobalt is reduced back to the 2+ oxidation state, the crosslink between amines began to break and protein-drug conjugate degraded to release free drug in its original form.[22] This process facilitated the stimuli responsive release of the drug inside cancer cells due to the higher amounts of reduced glutathione inside the cells compared to extra cellular space.[17]

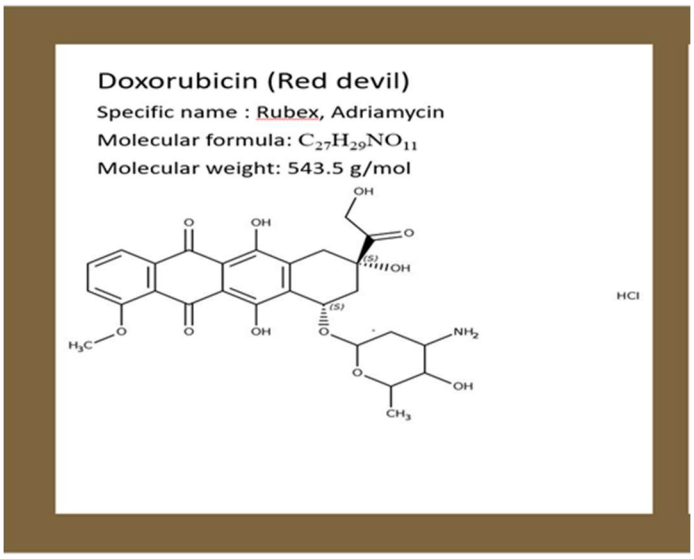

Figure 3. Chemical structure of Doxorubicin.[26]

Various other strategies are known for triggering release of encapsulated anti-cancer drugs. One of the alternative methods is to produce the reduced environment that would participate in the release of adenosine triphosphate (ATP) by an active targeting and stimuli responsive drug delivery.[22] Other triggered release formulations have been designed that rely on external triggers (magnetic field, light, heat) or internal ones (pH, enzymatic action) to release therapeutics. SERS (Surface Enhanced Raman Spectroscopy) can be used to probe drug loading for formulations that contain gold nanoparticles, which rely on light and/or plasma resonance absorption. Infrared light can also be used to trigger drug release at specific locations in the body.[27] Another similar approach utilized heat sensitive liposomes containing drug.[27] The heat from the surrounding environment in the body forces an active drug to release from the liposomes.[27] The release of drugs showed conclusive evidence of higher amount of drug intake and the concurrent penetration of drug into the cancerous/tumor cells. Another popular class of delivery vector is drug-antibody conjugates. These constructs can display a very high level of specificity in terms of targeting the delivery of the drug with rapid release of the drug in tumor cells. While a high level of bioavailability of drug is often observed, in some cases this strategy has also exhibited higher amounts of off-target

toxicity.[28,29,30] Doxorubicin-albumin conjugation efficiency is examined using several methods discussed below.

Analytical Techniques

Dialysis Experiments

The amount of Doxorubicin bound to protein was determined through dialysis experiments. The dialysis cassettes that were used had a 3500 MWCO (molecular weight cut off). With a molecular weight of ~600, dox will diffuse freely through the membrane; however, albumin (~67 kDa) cannot. For these experiments, reactions (less than 3 mL total volume of solution) run in vials to perform the conjugation chemistry were transferred to dialysis cassettes. The cassette was then be dialyzed in 200 mL phosphate buffered saline (PBS). One can use any other buffer solutions that falls in a pH range from 7.0 to 7.4 such as tris buffered saline solution. Any unbound Doxorubicin will diffuse out of the cassette over time until an equilibrium is established with the concentration inside the cassette is equal to that in the bulk phase. The initial purpose of the research was to obtain a fusion of albumin (protein) and doxorubicin prodrug. Figure 4 shows the chemical substances that are required at an initial reaction stage.

Figure 4. Stock solutions routinely utilized.[31]

HSA (100 mg) was added to a 15 mL plastic centrifuge tube containing 10 mL of ultrapure water. The solution was mixed thoroughly by vortexing to ensure all protein is dissolved (about 5 min). Stock Doxorubicin solutions (5 mg/mL) were prepared by a member of my research team with more experience because the compound is highly toxic. The entire contents of a single bottle (200 mg) were dissolved in 40 mL ultrapure water and then aliquoted in 1 mL samples in individual Eppendorf tubes. These individual samples were kept frozen and then used, as necessary. Cobalt chloride solution was prepared by mixing 0.238 mg of cobalt chloride into 1 mL of ultrapure water (see Figure 4).

For each reaction, the solutions of Doxorubicin and human serum albumin were mixed, and the pH of this solution was adjusted to pH 10 using a sodium hydroxide solution. Both the Doxorubicin and albumin possess amine group(s) in their chemical structures. Raising the pH ensured that the amine group(s) were in the deprotonated form, which facilitates the reaction of

the amines with cobalt. After each reaction, the solution from each vial was transferred to dialysis cassettes and dialyzed in a 200 mL aqueous solution. Samples from the bulk phase for each set of reaction conditions were taken every 24 hours for up to 72 hours. Quantification of unbound Doxorubicin in the bulk phase was examined via High Performance Liquid Chromatography (HPLC).

HPLC Analysis

For our research, HPLC was used to quantify the amount of Doxorubicin released from the dialysis cassette into the bulk PBS solution. HPLC is an analytical tool that works on the principle of the separation all the chemical components from a reaction mixture. HPLC instruments are equipped with high pressure pumps. The pumps induce the solvent (mobile phase) with the analyte to pass through the column (stationary phase). The stationary phase in the columns is made up of resins. The column separates each component of the mixture based on interaction of each component with the resin, which is based on polarity. The instrument used in these studies was a reverse phased HPLC. In this scenario, the mobile phase was a polar solution, and the stationary phase was a nonpolar one. The increased interaction of a particular compound with the resin resulted in a longer retention time (elution). Conversely, the compounds interacting less with the resin were eluted faster. The mobile phases can either be a single solution or a mixture of two or more liquids. Many analytes possess both polar and nonpolar groups in their chemical structure. Making a choice of a stationary phase and mobile phase is a key factor for the efficiency of separation in HPLC instruments. The mobile phase used here was a premixed of solution and employed an isocratic flow. Our mobile phase was a mixture of water and acetonitrile with a ratio of 70:30 water and acetonitrile. The pH of the water was first adjusted to a value of 3 using phosphoric acid. A non-polar C-18 column (composed of alkyl-chained carbon skeleton) was used

as a stationary phase. Our protocol was optimized using dox solutions of known concentration. The HPLC instrument was equipped with both a UV-visible and fluorescence detectors. The HPLC instrument can also be equipped with various other detectors like chemiluminescence, and other detectors depending on the need (limit of detection). Each separated component of mixture passed through UV visible detector where the quantification was achieved based on the amount of signal observed. The maximum absorption of Doxorubicin in a UV visible region occurs at 233 nm and at 253 nm. The cobalt complexes were easily separated because they are highly polar and therefore interacted little with the stationary phase. Dox and cobalt exhibit absorbance maximums in the UV visible region, so it was very important that doxorubicin and cobalt could be separated before detection. A calibration curve was generated using Doxorubicin solutions of known concentration. These samples were obtained by adding just Doxorubicin to a dialysis cassette and then monitoring the bulk phase. A series of dilutions from this sample were prepared and analyzed by HPLC. The integrated peak area for each sample was then plotted vs. concentration and a linear curve fit applied. The equation from this line was used to determine concentrations of unknown samples by inputting the integrated peak area and then solving for concentration. The concentration of Doxorubicin from these samples was used to determine the number of Doxorubicin molecules bond to a protein for each experiment.

Dynamic Light Scattering

Dynamic light scattering (DLS) is an analytical is an analytical tool that can be used to observe the protein aggregation. DLS was used to determine the particle size distribution of a liquid medium with a sensitivity of as low as 1 nm in size. The instrument was equipped with a laser light that falls on a sample. The difference between the initial laser beam and the scattered light was used to measure the particle size that can be detected by a photon detector placed at a

certain angle. DLS was used for our experiment to determine the stability of Dox – HSA stability in the solution. Many proteins can exhibit aggregation with changes in solution pH and composite. Generally, protein aggregation must be avoided when making various pharmaceutical products.

DLS uses the electronic field of the light. DLS uses Brownian motion to determine the velocity distribution of the particles in a liquid which is related to particle size. The DLS instrument uses a laser diode, which is coupled to the sample solutions via an optical probe/power splitter. As soon as a beam of the laser strikes the sample, the light gets reflected, refracted, or scattered. The scattered light then falls on to the fluid interface and it ultimately reaches the photodetectors. The scattering after interacting with the sample solution is referred to as doppler shifted light. The output detection signal is enhanced via a photomultiplication detection system known as Heterodyne detection.

Differential Scanning Calorimetry

The synthesized drug-protein (Doxorubicin-HSA) conjugate, polymerized via cobalt crosslinking, was further analyzed by Differential Scanning Calorimetry (DSC). DSC is a technique that is used to observe changes in the thermodynamic stability. It can be used to determine the change in heat (enthalpy), which is linked with the thermal denaturation of the proteins. The parameter that is measured by DSC is thermal transition temperature (T_M or melting temperature). T_M is the temperature where the protein is 50% denatured and 50% in its native state. The larger the T_M value, the more the stable the protein is. An appropriate buffer solution was used in which the drug-protein conjugates were added. The same buffer was used separately as a reference solution. The area under the curve obtained from the peak is a total change in heat required to unfold (denature) the protein. The breaking of non-covalent hydrogen bonding, which are responsible for maintaining the proper tertiary structure, is an endothermic reaction. For our

research, the thermodynamic stability of the drug protein conjugate was investigated at all the stages (i.e., before and after addition of each parameter).

CHAPTER II

MATERIALS AND METHODS

High Performance Liquid Chromatography

Quantification of Dox bound/unbound to protein was conducted on a reversed phase HLPC instrument, Agilent Infinity II (see Figure 5). The instrument was composed of 4 subunits: an autosampler, an Agilent 1260 II high pressure pump, a double beam photometer detector with deuterium lamp (UV source) and an Open Lab ChemStation software. The determination of the number of molecules of Dox bound to a molecule of protein was made possible by determining the concentration of Dox bound (in μg) using a calibration curve, which was obtained using standard solutions. A calibration curve was generated each time before examining the effects of each parameter. The standards were placed in 2 mL glass vials, which were then placed in the vial tray that goes into the instrument. The instrument is equipped with an autosampler, so the process was automated. A stationary phase consisting of a non-polar C-18 Agilent Infinity II column was used to obtain satisfactory separation. For all the sample runs on low-pressure gradient, the pressure reading was typically about 1400 psi. The flow rate of the mobile phase was set to 1 mL/min. The run time for all the samples was set to 9 min as the peaks of interest were observed at around 2-4 min. A polar mobile phase with an isocratic type of elution was used. The mobile phase was a composition of an ultra-pure water and the HPLC grade acetonitrile with a ratio of 70:30. The pH of the water was brought down to pH-3 using phosphoric acid prior to mixing with acetonitrile. The mobile phase solvent was degassed for at least 15 min using a 3510 Branson sonicating device. Degassing a mobile phase ensured that the solvent was without any dissolved gas which could interfere with data collection. The HPLC instrument was run for at least 30 min to ensure there were no contaminants in the column that could be a source of extraneous peaks.

The sample aliquot was set to 20 µL/injection. The area under the curve was determined via the Open lab ChemStation software.

Figure 5. Photo of Agilent Infinity II HPLC instrument.

DLS

The determination of the overall stability of the synthesized drug -polymer conjugate was carried out using a Microtrac Nanotrac Wave II particle size and Zeta-potential Analyzer (Microtec Inc.; see Figure 6). In addition to the analysis of Zeta-potential and particle size determination, this optical instrument can also be used for molecular weight determination of a chemical substance. The Microtec FLEX software for Microsoft Windows 10 was used to interpret the analytical information provided by the Nanotrac Wave II instrument. For our research, the protein (or protein bound Dox complex) samples were used to determine the mean particle size of the protein. The samples were collected from the dialysis cassette after 72 hours dialyzing the sample in a 1X PBS solution or water. The samples were then analyzed using all the changing parameters including pH

(pH 7 to pH 10), different concentration of cobalt, and different concentration of Dox. All samples were homogeneously mixed using a vortex mixer before inducing them to the Nanotrac Wave II instrument. All samples were transferred to the instrument using a 3 mL Pasteur plastic pipette. The sample cell was rinsed by 0.5 mL of ultra-pure water before analyzing each sample. All samples were analyzed at room temperature with the instrument set to autozero function. An average size determination for each sample obtained by averaging six individual runs 30 seconds each. Two parameters, the polydispersity index (PDI) and the particle size distribution, were calculated using the Microtec FLEX software.

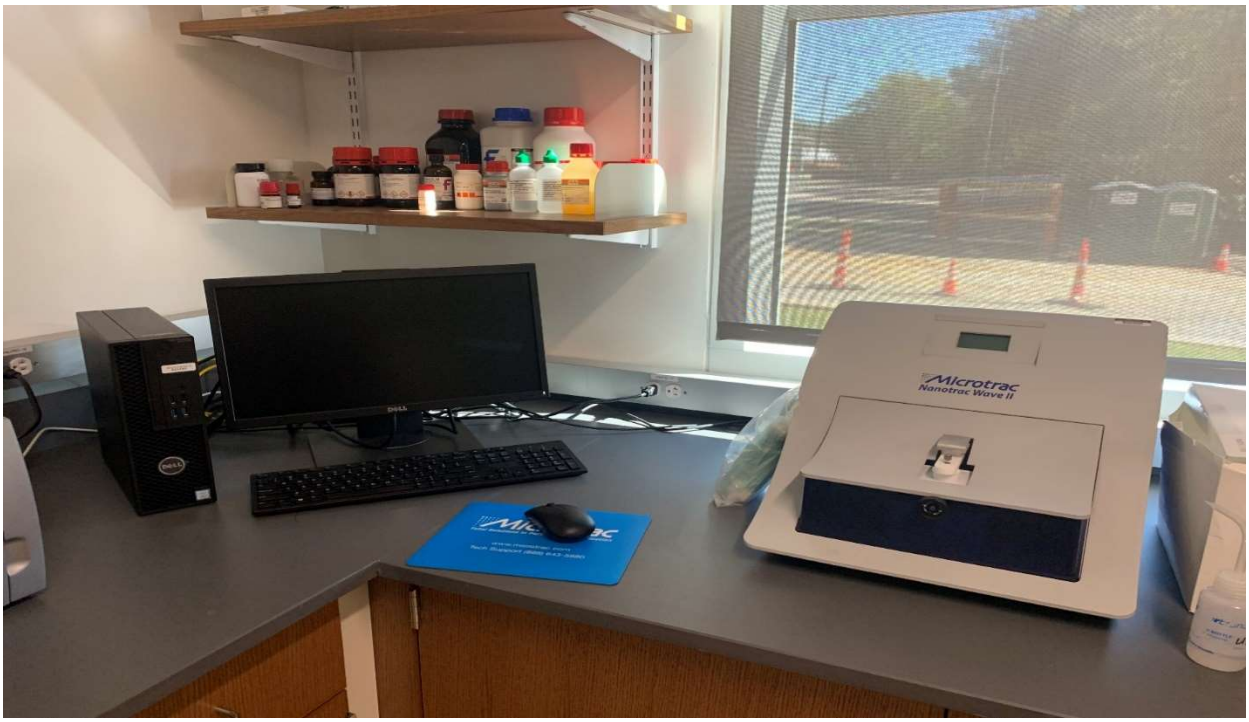

Figure 6. Photo of Microtrac Nanotrac Wave II particle size and Leta-potential Analyzer (Microtec Inc.) DLS instrument.

DSC

The overall stability of the protein was determined using 6100 Nano II CSC model Differential Scanning Calorimeter (see Figure 7). The accompanying software suite was used for data analysis. The heat that was measured in micro watts over the course of the experiment was used to calculate molar heat capacity as a function of temperature. The data obtained from the experiment was used to calculate the heat capacity using the known concentration of protein (4.4 mg/mL), HAS molecular mass (66.5 KDa), volume of solution used in the cells (around 750 μL), and the solvent only baseline thermogram (molar heat capacity versus the temperature). The baseline was first obtained by using a buffer solution containing all solution components except the protein as a reference. The sample was then analyzed using the same buffer as a reference versus the sample containing protein. This baseline was then subtracted from the thermograms obtained for each sample. The baseline-corrected thermogram showed the T_M peak for the protein. T_M (transition temperature) is the temperature at the highest peak of the thermogram. T_M is the temperature at which the protein began the denaturation process. The goal here was to determine the T_M of free HSA and compare that to the values for our conjugates. If the T_M value is lower for our conjugates, one could conclude that the conjugates are less stable than the native protein and the conjugation has destabilized the protein.

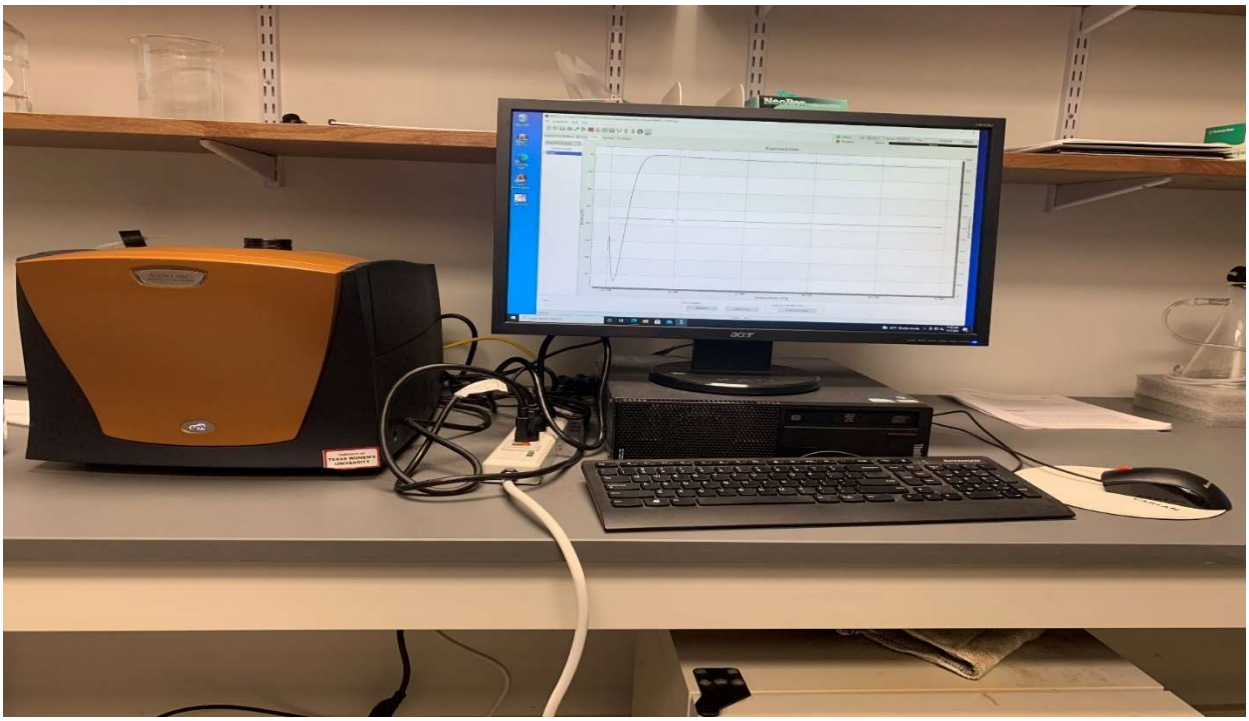

Figure 7. Photo of 6100 Nano II CSC model Differential Scanning Calorimeter instrument.

Synthesis of Doxorubicin-Albumin Prodrug Via Cobalt Crosslinking

Initial experiments to synthesize Dox-Albumin via cobalt crosslinking was performed by adapting the protocols from "Werner Complex Viewed Anew," by Doug T Ngugen et al."[22] The initial experiments led to a better understanding how to utilize cobalt's coordination chemistry as a crosslinking chemistry that could ultimately help us develop methodologies to synthesize stable drug-protein conjugate.

A stock solution of 0.1 M $CoCl_2.6H_2O$ (Fischer Scientific Lot #142533) was prepared in a 2 mL centrifuge tube. Typically, 0.0238 gm of $CoCl_2.6H_2O$ was added to a centrifuge tube followed by 1 mL of ultra-pure water. A 0.25 M NaOH solution was prepared in a 20 mL centrifuge tube by adding 0.10 g of NaOH pellets (GFS chemicals, Columbus, Ohio) followed by 10 mL of ultra-pure water. Similarly, a 10 mg/1 mL HSA was prepared adding 0.10 gm of HSA into a 20 mL centrifuge tube (MP Biomedicals LLC, Solon, OH, USA) and making a volume up to 10 mL

with ultra-pure water. Stock Doxorubicin solutions with a concentration of 5 mg/mL were prepared by adding 10 mg of Doxorubicin (Sigma Aldrich, St. Louis, Missouri) to a small Eppendorf of tube followed by 2 mL of ultra-pure water.

CHAPTER III

RESULTS AND DISCUSSIONS

Evaluation of Dox Concentrations with Different Reaction Conditions and Parameters

1) Constructing a Calibration Curve (HPLC Evaluation)

A calibration curve is a mathematical tool that can be used to find the concentration of a chemical substance with an unknown concentration. A calibration curve can only be obtained by using a chemical substance of a known concentration. The calibration curve was constructed in this research to obtain the concentrations of Dox in unknown solutions with varying reaction parameters.

An initial Dox solution with the concentration of 50 μg/mL of Dox was prepared and analyzed via HPLC. A peak for Dox was observed with an elution time of 4-5 minutes. A series of standard solutions of known concentration of Dox were analyzed via HPLC instrument to obtain the integrated peak area, which is directly proportional to concentration. The calibration curve was plotted as peak area (y-axis) vs the concentration of standard Dox solutions (x-axis) using Microsoft Excel software. The slope equation was obtained through a linear data fit, which affords a trend line that allowed us to determine the concentration of unknown Dox samples simply by the peak area. All the calibration cure samples were made from dialyzing 52.5 μL of 5 mg/mL Dox for 72 hours in 200 mL of 1X PBS (or other bulk phase from the experiment). A series of dilutions with the ratio of 1:0, 1:3, 1:6, and 1:10 were prepared using 1X PBS solution. A series of calibration standards were prepared for each experiment and run alongside the unknown samples on the same day.

The concentration of unknown Dox sample solutions (X) was determined using a slope equation: $y = mx+c$

- Where y= value of the area under the curve obtained from HPLC
- m= slope
- c= y intercept
- X was determined by rearranging the slope formula
- X= y-c/m

2) Effect of Reaction Time Using The Bulk Phase of PBS for Dialysis

The effect of reaction time before addition of hydrogen peroxide was examined to determine if it impacted overall binding of the drug to the protein. A total of five samples were: Sample 1 was the Dox only control for constructing the calibration curve. Sample 2, 3, and 4 contained Dox, HSA, cobalt, and hydrogen peroxide. The only difference between samples 2-4 was reaction time prior to the addition of hydrogen peroxide with an interval of 10 min, 1 hour, and 4 hours, respectively. Sample 5 contained all the same reagents as 2-4, but without cobalt. Samples were collected from the bulk phase after 72 hours and analyzed via HPLC. A series of dilutions were made from sample 1, which was analyzed via he HPLC to generate a Dox calibration curve. Dialyzing was performed for 72 hours in PBS under the assumption that all the unbound/free Dox from each cassette would have into the bulk phase.

During the initial experiments, the binding of Dox to HSA was not successful. The reaction solution had an initial pH of around 5 to 6, which was too low to afford appreciable amounts of the deprotonated amine needed for crosslinking. Dox is soluble at this pH; however, when the solution was adjusted to pH 8 thorough addition of sodium hydroxide, a precipitate formed. Therefore, separate solutions of Dox and protein were prepared. Previous studies have shown that the addition of cobalt after adjusting the pH of the reaction mixture to pH 8 showed maximum binding of Dox molecules to the

protein. So, for this experiment, the addition of cobalt was carried out after the Dox and HSA solutions were adjusted to pH 8.

After the appropriate reaction times, the samples were transferred to dialysis cassettes and were then placed in the 200 mL PBS with a Styrofoam holder attached to each cassette. The samples were dialyzed for 72 hours at which point 1 mL of each bulk phase was transferred to HPLC vial. A series of dilutions in the ratio of 1:10, 1:6, 1:3, and 1:0 was made from the bulk phase of sample 1 using PBS as a diluent in order to generate a calibration curve (see Figure 8). The sample solutions contained within the dialysis cassette from samples 2, 3, and 4 were collected via the syringe and transferred to separate vials. The size of the conjugates within the dialysis cassette was further investigated via DLS. All Dox waste was transferred into the designated waste container.

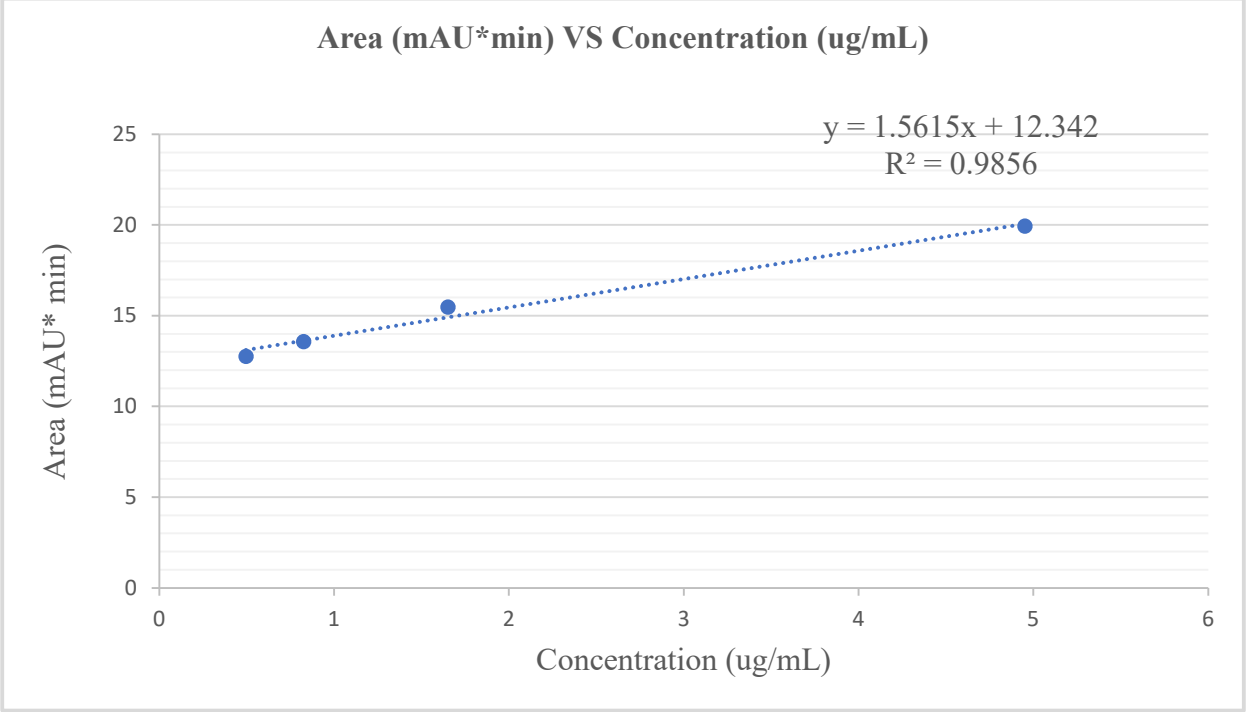

Figure 8. Calibration curve- Area (mAU* min) VS Concentration (ug/mL) for effect of reaction time experiments.

Table 1. Standard solutions of Dox displaying concentration and area under the curve obtained via HPLC.

Solutions	conc (ug/ml)	Average area
1:10 (0.495ug/ml)	0.495	12.76666667
1:6 (0.825ug/ml)	0.825	13.56666667
1:3 (1.65ug/ml)	1.65	15.46666667
undiluted (4.95ug/ml)	4.95	19.93333333

Table 2. HPLC results for the effect of reaction time.

Reaction time	Mean Area	unknown conc (ug/mL)	amount in bulk ug	amount retained in cassette ug	% Retained	moles of DOX retained	# DOX molecules/ molecule of HSA
sample 2 (10 min)	18.5	3.94364	796.61	153.38	16.1456	2.6E-07	1.759575
sample 3 (1 hour)	18.5	3.92226	792.30	157.69	16.599	2.7E-07	1.809042
sample 4 (4 hours)	27.3	9.60059	1939.3	-989.32	-104.13	-1E-06	-11.3492
sample 5 (10 min- no cobalt)	20.3	6.51595	1316.2	-366.22	-38.549	-6E-07	-4.20121

The maximum binding of Dox to HSA was found to be 1.8 molecules of Dox per each molecule of HSA in sample 3 with a reaction time of 1 hour, followed by sample 2 with 1.76 molecules at a reaction time of 10 min. The reaction mixture in the sample 5 with no cobalt showed that it had released more Dox than was added according to the calibration curve. This was later attributed to precipitation of Dox inside the cassette for all samples, especially the Dox-only control sample (see Tables 1-2). We could see no correlation in the number of Dox molecules bound per HSA as a function of reaction time (see Figure 9).

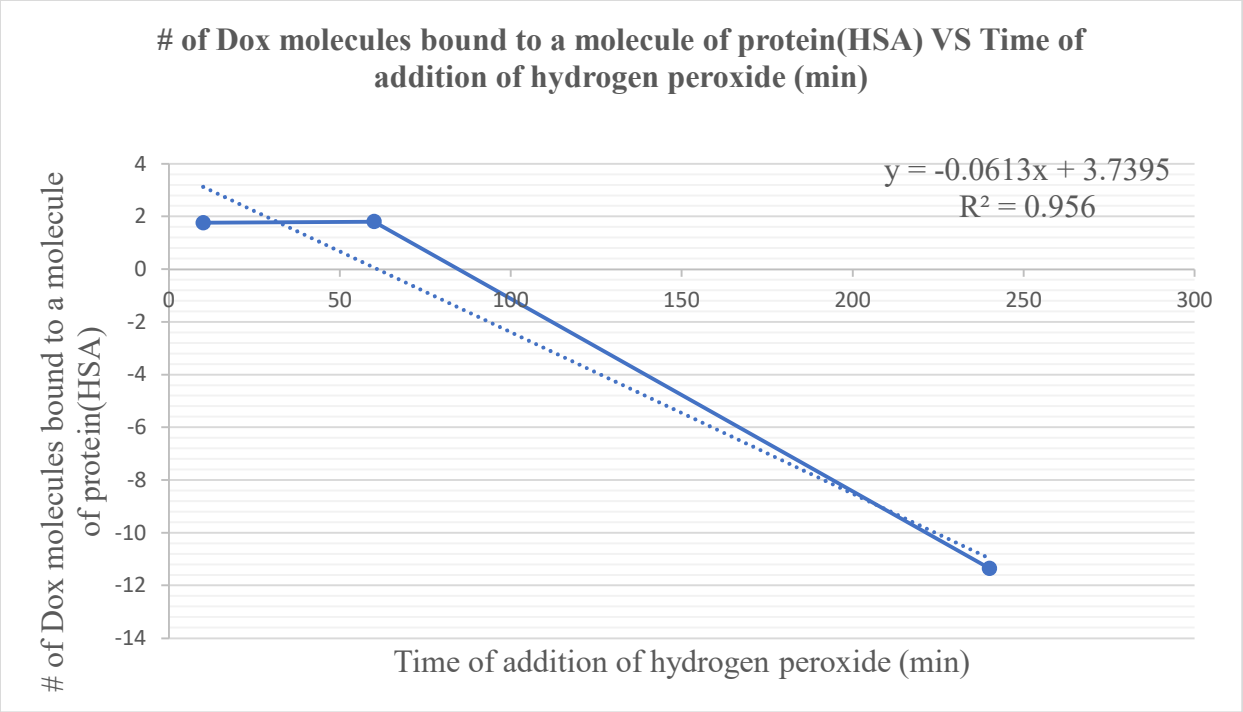

Figure 9. Graph representing # of DOX molecules/ a molecule of HSA VS reaction time (min).

3) Formation of Dox Precipitates Through Dimerization

According to Yuji Yamada, Dox begins to precipitate once it encounters buffers like, phosphate buffered saline.[32] Dox was also shown to precipitate in solutions containing certain drugs like Heparin.[33,34] It did not exhibit any precipitation when dissolved in ultra-pure water. Daunorubicin, on the other hand, which is a 14-dehydroxylated form of Doxorubicin exhibited no precipitation when dissolved in buffers or water.

Dox containing PBS solutions were initially clear, but was reported to slowly start forming precipitates when incubated for 24 hours at a temperature of 37 °C.[32] About 90% of the Dox was reported to precipitate after incubation for 24 hours at 60 °C. The rate of precipitation was reported to increase with increasing pH. All subsequent experiments described in this thesis utilized ultra-pure water as the bulk phase for dialysis.

The proposed mechanism of precipitation was through the dimerization of the Dox via an alpha hydroxy ketone which undergoes keto-enol tautomerization. The tautomerization produces an alpha-hydroxy aldehyde. The alpha-hydroxy aldehyde forms alpha-hydroxy imine with a second molecule of Dox. The alpha-hydroxy imine undergoes imine-enamine tautomerization to form an enaminol. Finally, the oxidation of enaminol produces alpha-iminoketone. All subsequent experiments described in this thesis utilized ultra-pure water as the bulk phase for dialysis.

3a) Effect of Reaction Time Using Ultra-Pure Water as The Bulk Phase

The effect of reaction time before addition of hydrogen peroxide was examined to determine if it impacted overall binding of the drug to the protein. A total of four samples were prepared. For sample 1 and 2, 200 μL of Dox, 1 mL of ultra-pure water, and 52.5 μL of 0.1 M cobalt chloride were added to a vial. Sodium hydroxide (10 μL of 0.25 M) was then added. HSA (1 mL of 10 mg/mL) was then added immediately to the vial. The only difference between sample 1 and sample 2 was the reaction time. For sample 1, hydrogen peroxide was added 10 min after the addition all other reagents, and for sample 2, hydrogen peroxide was added after 4 hours. Sample 3 contained 1 mL of 10 mg/ml HSA solution plus 1.255 mL of ultra-pure water. Sample 3 was prepared as a control for the evaluating of the stability of the protein through DSC experiments. Sample 4 was prepared to generate a calibration curve for Dox. Sample 4 contained the same amounts of Dox, cobalt, and water as sample 1, the only difference between them was that 1 additional mL ultra-pure water was added instead of 1 mL of protein. Because sample 4 did not contain protein, it was expected that all the Dox added would diffuse into the bulk phase. All samples were injected into pre-hydrated dialysis cassettes. The cassettes were then placed in the 200 mL of ultra-pure water with a Styrofoam holder attached to each cassette. The samples were incubated for 72 hours at room temperature. After incubation, 1 mL of each bulk phase was

transferred to HPLC vial. A series of dilutions in the ratio of 1:10, 1:6, 1:3, and 1:0 was prepared from the bulk phase of sample 4 using ultra-pure water as the diluent to obtain a calibration curve (see Figure 10). The solutions within the dialysis cassette from samples 1, 2, and 3 were transferred via syringe to vials for future analysis by DLS and DSC. The size of the conjugates was evaluated using DLS. All Dox waste was transferred into the designated waste container.

Table 3. Standard solutions of Dox displaying concentration and area under the curve obtained via HPLC.

Solutions	conc (ug/ml)	Average area
1:10 (0.495 ug/mL)	0.495	3.15
1:6 (0.825 ug/mL)	0.825	5.1
1:3 (1.65 ug/mL)	1.65	12.85
undiluted (4.95 ug/mL)	4.95	56.35

Table 4. Results for the effect of reaction time using ultra-pure water as the bulk phase.

Reaction time	Mean Area	unknown conc (ug/mL)	amount in bulk ug	amount retained in cassette ug	% Retained	moles of DOX retained	# DOX molecules/ molecule of HSA
Sample 1- 10 min interval	25.85	2.51034	507.0886	442.91131	46.622	7.6E-07	5.08094
Sample 2- 4 hours interval	29.2	2.78416	562.4017	387.59825	40.799	6.6E-07	4.44641

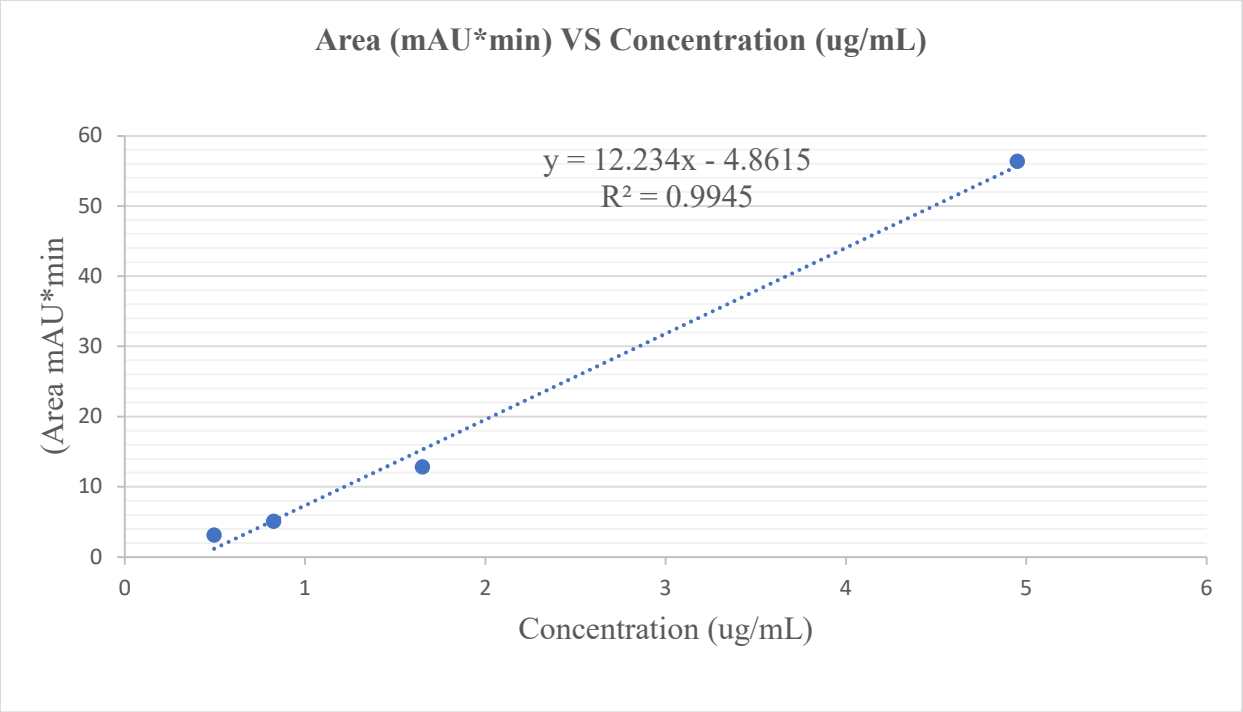

Figure 10. Calibration curve- Area (mAU* min) VS Concentration (ug/mL) for effect of reaction time using ultra-pure water as the bulk phase.

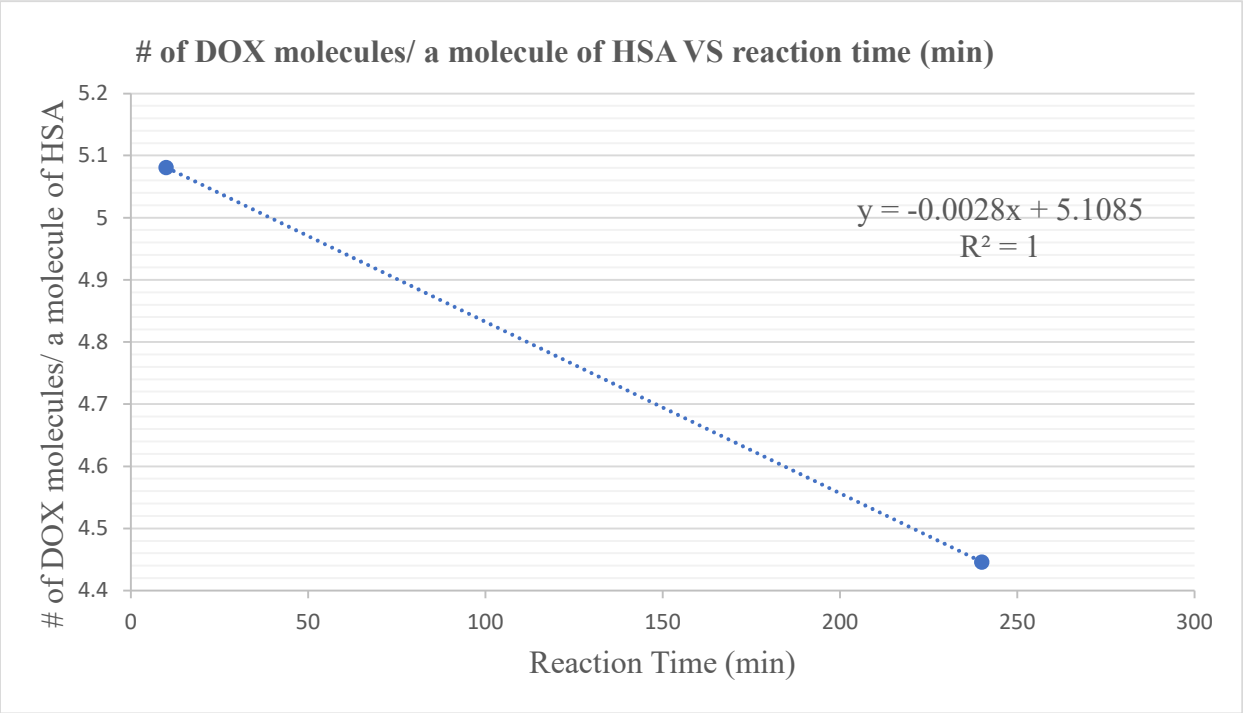

Figure 11. Graph representing # of DOX molecules/ a molecule of HSA VS Reaction time (min).

HPLC analysis revealed that sample 1 retained more Dox inside the dialysis cassette compared to sample 2; however, only a small difference was noted. For sample 1 with 10 min reaction time, each HSA molecule had bound 5.08 molecules of Dox. For sample 2 with a 4-hour reaction time, each HSA molecule had bound 4.45 Dox molecules (see Figure 11). This experiment demonstrates that the conjugation chemistry is rapid and that a 10 min reaction time is sufficient for the cobalt-induced amine crosslinking to occur (see Tables 3-4).

3b) Effects of pH Using Ultra-Pure Water as The Bulk Phase

This experiment was designed to determine the effect of pH on drug-protein conjugation, which could be an important factor in this research. The pKa for a protonated amine is 9-10, so at neutral pH all the amines would be in their protonated state. The cobalt coordination chemistry requires the deprotonated state; thus, it was expected that raise the pH would increase the amount of crosslinking and ultimately the number of Dox molecules per protein. For this experiment, a total of 3 samples were prepared. One at pH 8, one at pH 9, and one to generate the calibration curve. For sample 1, 1 mL of 10mg/mL of Human Serum Albumin was added to a vial. The pH was measured and adjusted pH 8 using 0.25 M NaOH. In a separate vial, 200 µL of 5 mg/mL Dox was added. Ultra-pure water (1 mL) was added to the vial followed by 52.2 µL of 0.1 M cobalt chloride solution. NaOH (10 µL of 0.25 M) was added, followed immediately by adding the pH adjusted protein solution. After a 10 min reaction time, hydrogen peroxide was added, and the solution was transferred to a pre-hydrated dialysis cassette. Air bubbles were removed using a syringe. The cassette was then placed into 200 mL of ultra-pure water, with a Styrofoam holder attached to the cassette. Sample 2 was prepared in the same manner as sample 1 with the only difference being that the pH of the protein solution was adjusted to 9 instead of 8. Sample 3 was a control sample that was used to obtain the calibration curve with a composition like the other

samples. The only difference was that it did not contain any protein solution where 1 mL of ultra-pure water was used as a substitute for the protein solution. The samples were incubated for 72 hours after which 1 mL of the bulk phase for each sample was transferred to HPLC vial. A series of dilutions in the ratio of 1:6, 1:3, and 1:0 was prepared from the bulk phase of sample 3 using ultra-pure water as the diluent to generate a calibration curve (see Figure 12). The sample solutions from within the dialysis cassette for samples 1 and 2 were transferred to vials using a syringe. The size of the conjugates within the dialysis cassette was investigated via DLS. All Dox waste was transferred into the designated waste container.

Table 5. Standard solutions of Dox displaying concentration and area under the curve obtained via HPLC.

Solutions	conc (ug/ml)	Mean area
1:6 (0.825ug/ml)	0.825	12.45
1:3 (1.65ug/ml)	1.65	17.85
undiluted (4.95ug/ml)	4.95	84.1

Table 6. Results for the effect of pH using ultra-pure water as the bulk phase.

Samples with different pH	Mean Area	unknown conc (ug/mL)	amount in bulk ug	amount retained in cassette ug	% Retained	moles of DOX retained	# DOX molecules/ molecule of HSA
Sample 1- pH 8	51.8	3.22825	652.1071	297.89282	31.3571	5.13626E-07	3.4173389
Sample 2- pH 9	28.2	1.92747	389.3508	560.64981	59.0157	9.66671E-07	6.4316097

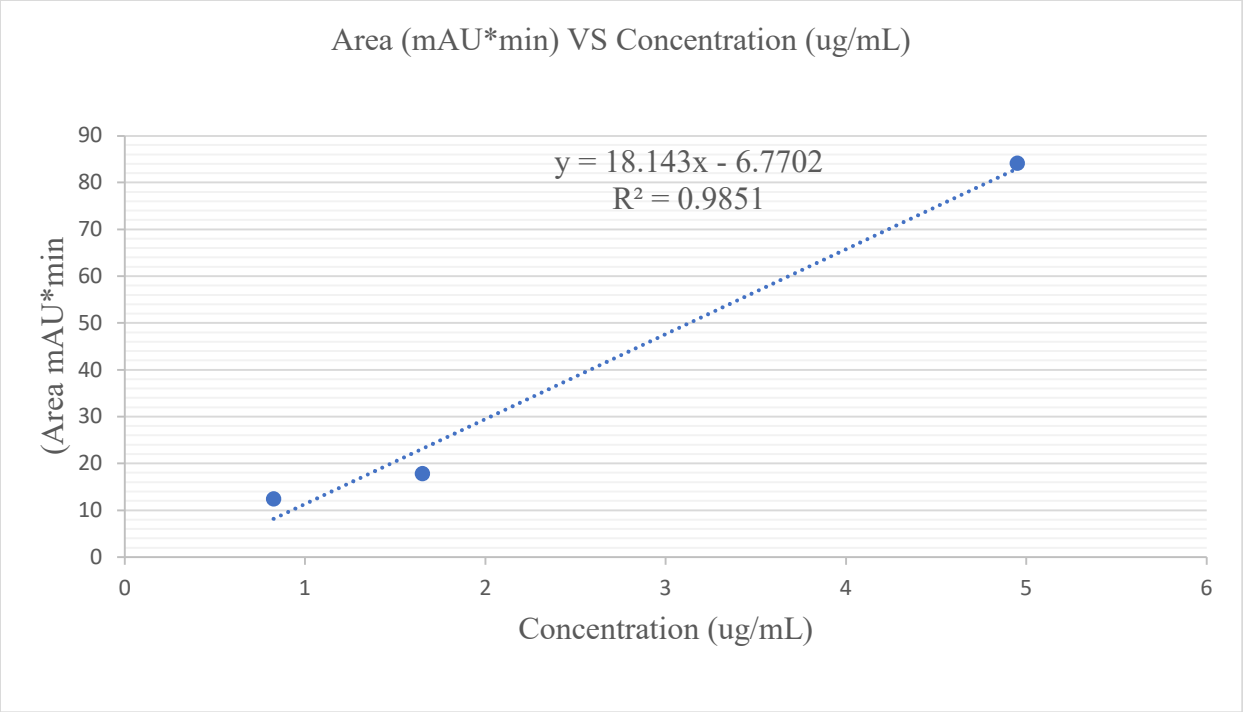

Figure 12. Calibration curve- Area (mAU* min) VS Concentration (ug/mL) for the effects of pH using ultra-pure water as the bulk phase.

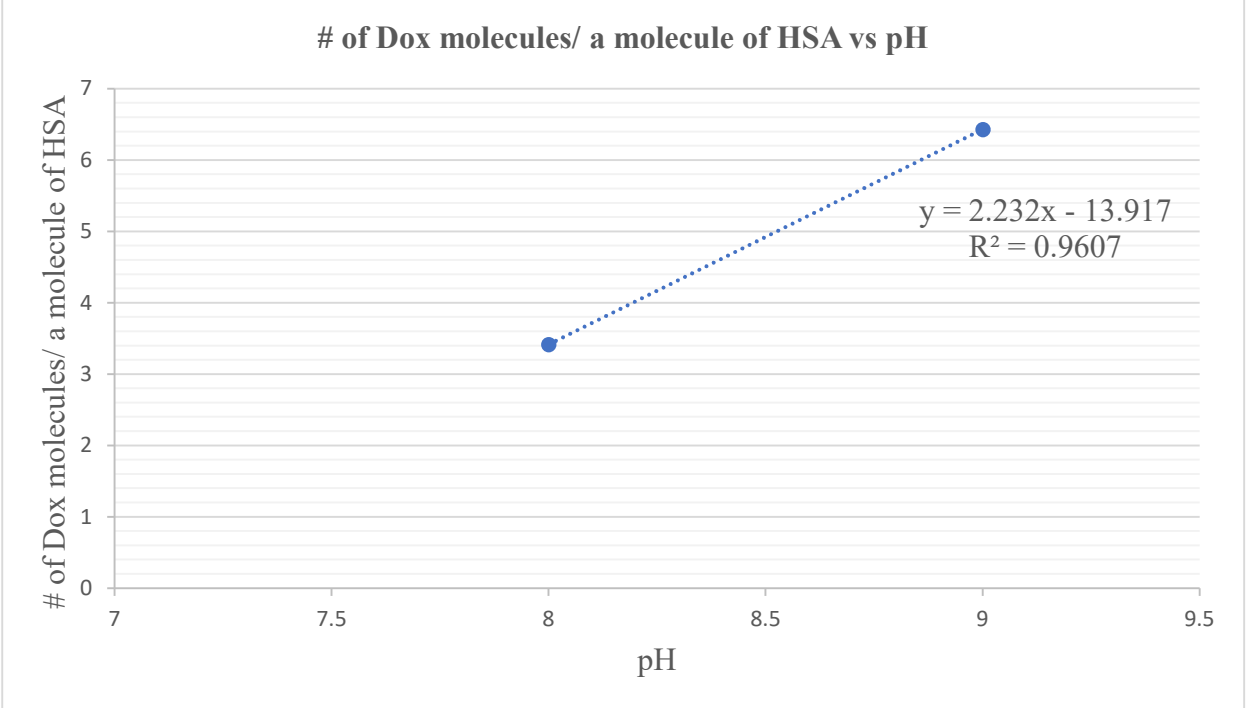

Figure 13. Graph representing # of DOX molecules/ a molecule of HSA VS pH.

HPLC analysis revealed that sample 2 retained the maximum amount of Dox in the dialysis cassette as expected. Sample 1 had 3.4 Dox molecules bound per protein molecule and sample 3 had 6.4 Dox molecules bound per protein molecule (see Tables 5-6). This experiment demonstrated that raising the pH leads to higher conjugation efficiency as expected (see Figure 13).

4) DLS Evaluation

DLS was used to examine samples for potential protein aggregation, which would be undesirable. DLS was conducted on samples taken from inside each dialysis cassette. Samples were vortexed for 1-2 min before transferring them into the instrument sample cell. DLS was be used to determine the mean size distribution of the protein in solution. If aggregation were to occur, the mean size distribution would be expected to increase. Mathematical tools like mean diameter, standard deviation, polydispersity index, 10% and 95% percentiles were taken in consideration to determine the monodispersity. Particle size distributions were found to be relatively uniform.

4a) Effect of Reaction Time Dialyzed in PBS

All samples displayed no protein aggregation as demonstrated by their uniform sizes. Sample 2, with a 10 min reaction time exhibited the lowest standard deviation (see Figures 14-17). The smallest mean diameter was 3.96 nm for sample 3, where the reaction time was 1 hour. The largest mean diameter was 4.73 nm for sample 3. The smallest 10% percentile passing was 2.960 for sample 3. The smallest 95% percentile was 6.77 for sample 2. The largest 10% and 95% percentile was found to be 3.63 and 7.67, respectively for sample 4 where the standard deviation was the highest (see Table 7).

Reaction time	Mean diameter of nanoparticle(nm)	Standard Deviation	Polydispersity Index	10% (nm)	95% (nm)
Sample 2 10 min	4.4	1.120	0.828	3.46	7.21
Sample 3 1 hour	3.96	1.130	0.855	2.960	6.77
Sample 4 4 hours	4.73	1.230	1.177	3.63	7.67
Sample 5 10 min + no cobalt	4.64	1.160	0.645	3.60	7.42

Table 7. The DLS data for effect of reaction time using 1X PBS solution as a dialyzing medium.

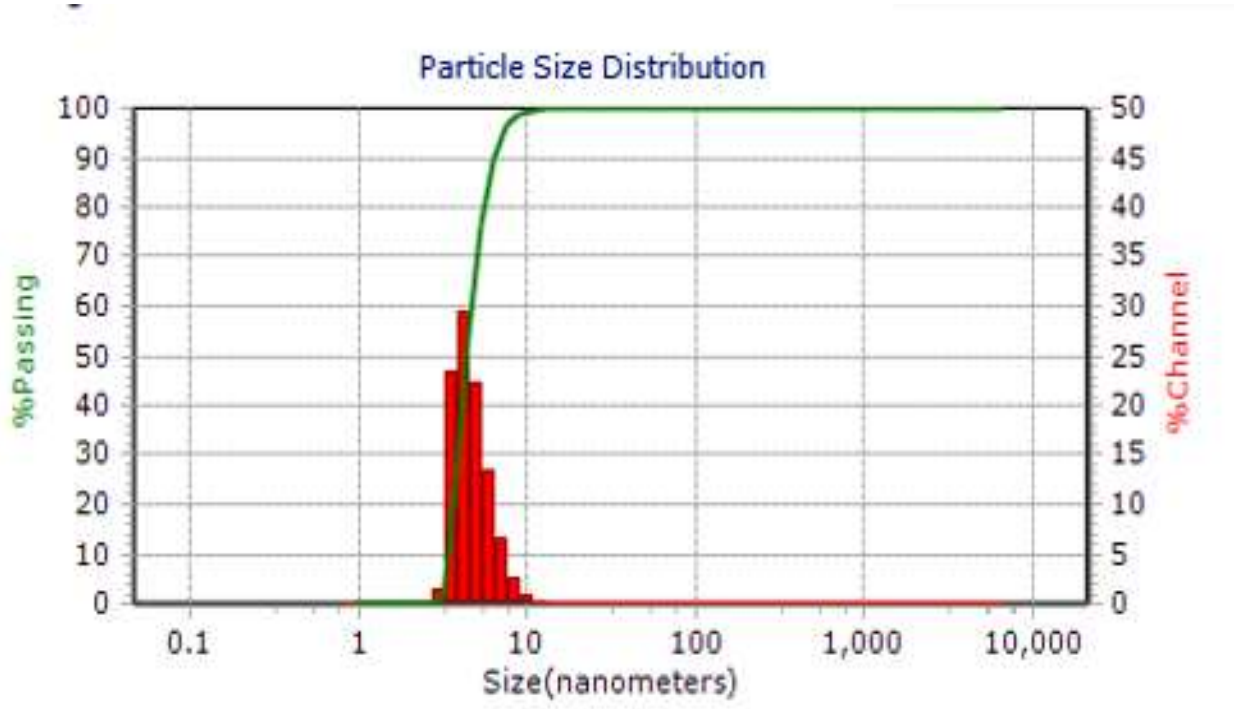

Figure 14. DLS graph for sample at 10 min reaction time.

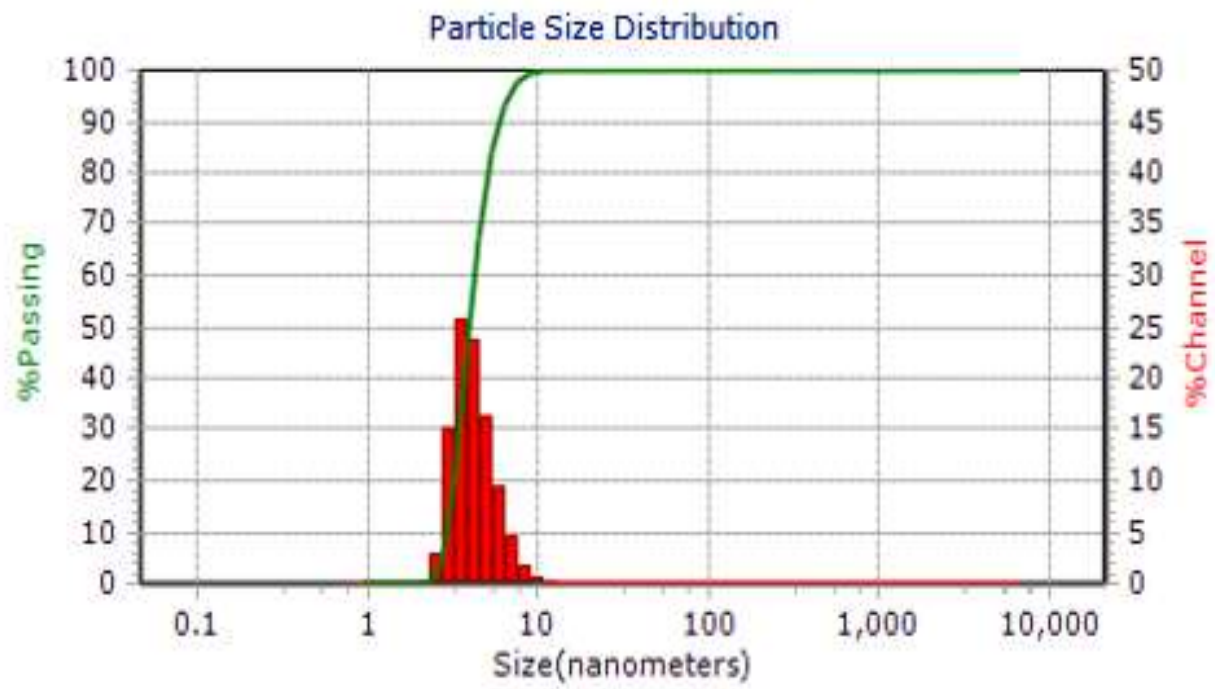

Figure15. DLS graph for sample at 60 min reaction time.

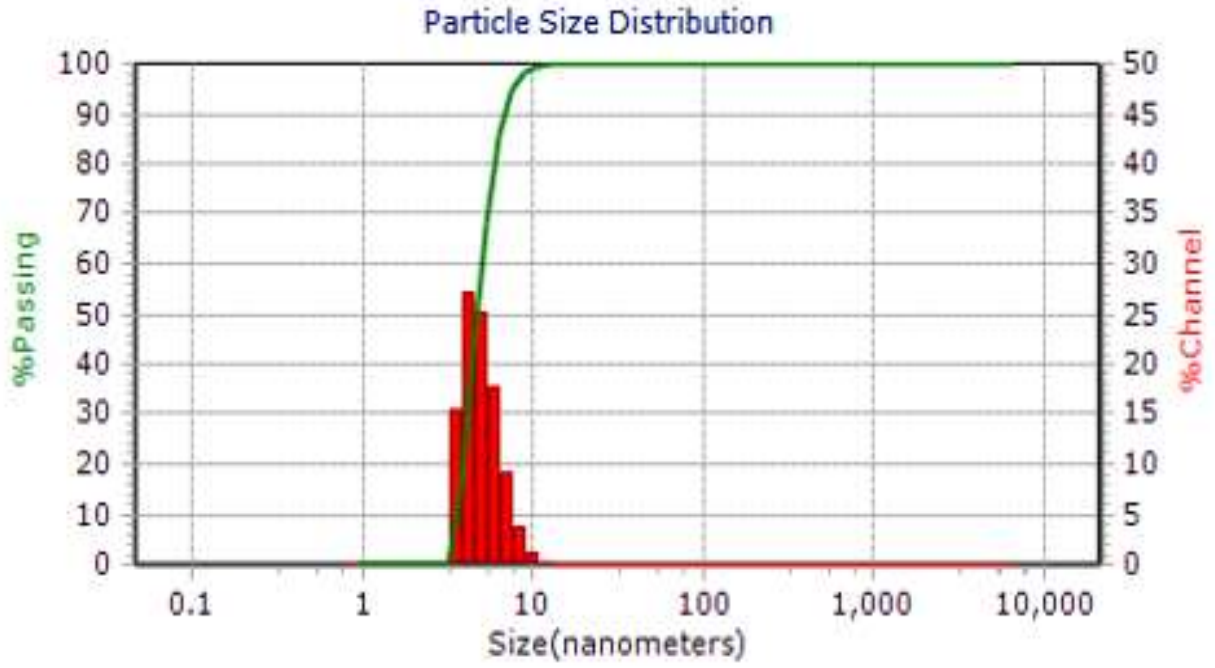

Figure 16. DLS graph for sample at 240 min reaction time.

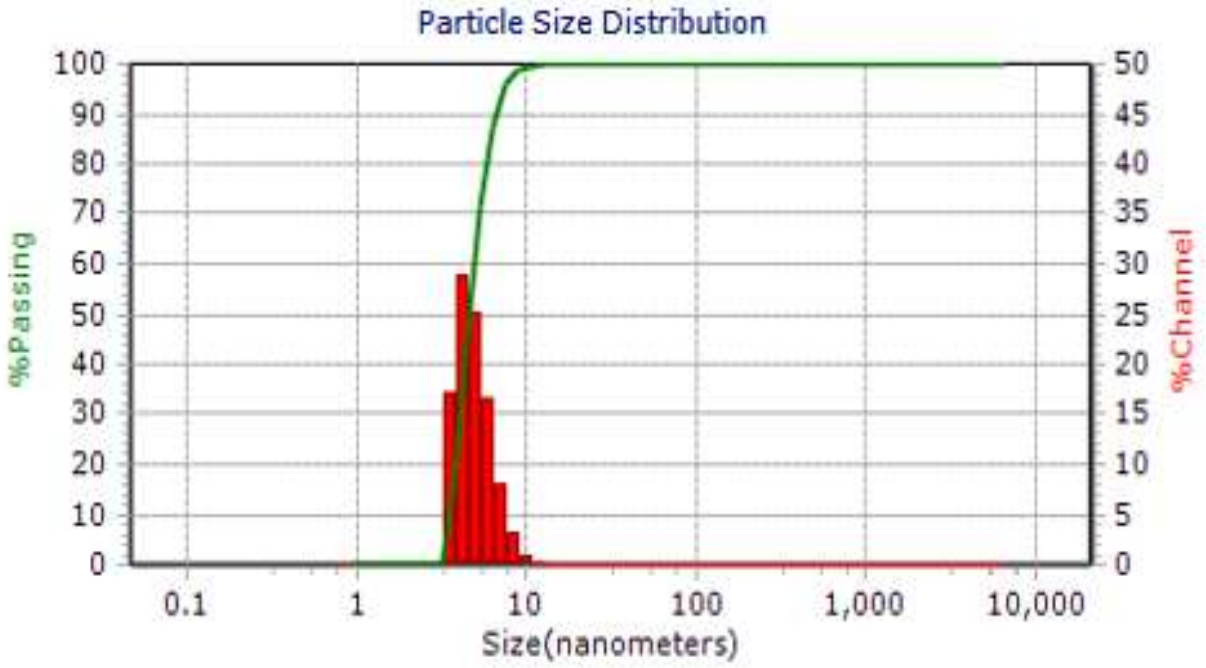

Figure 17. DLS graph for sample at 10 min reaction time with no cobalt.

4b) Effect of Reaction Time Using an Ultra-Pure Water as The Bulk Phase

This set of experiments afford the benefit of having a sample that contained only protein, which could be used in comparing the results with those of the conjugates (see Figures 18-20). The protein only control resulted in a mean size of 2.87 nm and polydispersity of 0.471. Sample 1 with a 10 min reaction time displayed the smallest size, with a mean diameter of 1.93 nm and the largest was from sample 3 (2.87 nm). When comparing protein only (see Figure 20) to the conjugate containing samples there was a clear difference in the shape of the size distributions. The protein only exhibits a Gaussian distribution whereas the conjugate samples appeared truncated on the lower end of the distribution and extend out further on the higher end. The range of the 10% and 95% confidence intervals was also narrower for the protein only control (see Table 8). These results indicate that some aggregation maybe occurring and will be the focus of future studies

Table 8. The DLS data effect of reaction time using ultra-pure water as the bulk phase

Reaction time	Mean diameter of nanoparticle (nm)	Standard Deviation	Polydispersity Index	10% (nm)	95% (nm)
10 min	1.93	0.990	0.496	1.270	5.28
4 hours	2.55	1.430	0.2842	1.790	7.73
protein + ultra-pure water (for DSC)	2.87	0.730	0.471	2.210	4.58

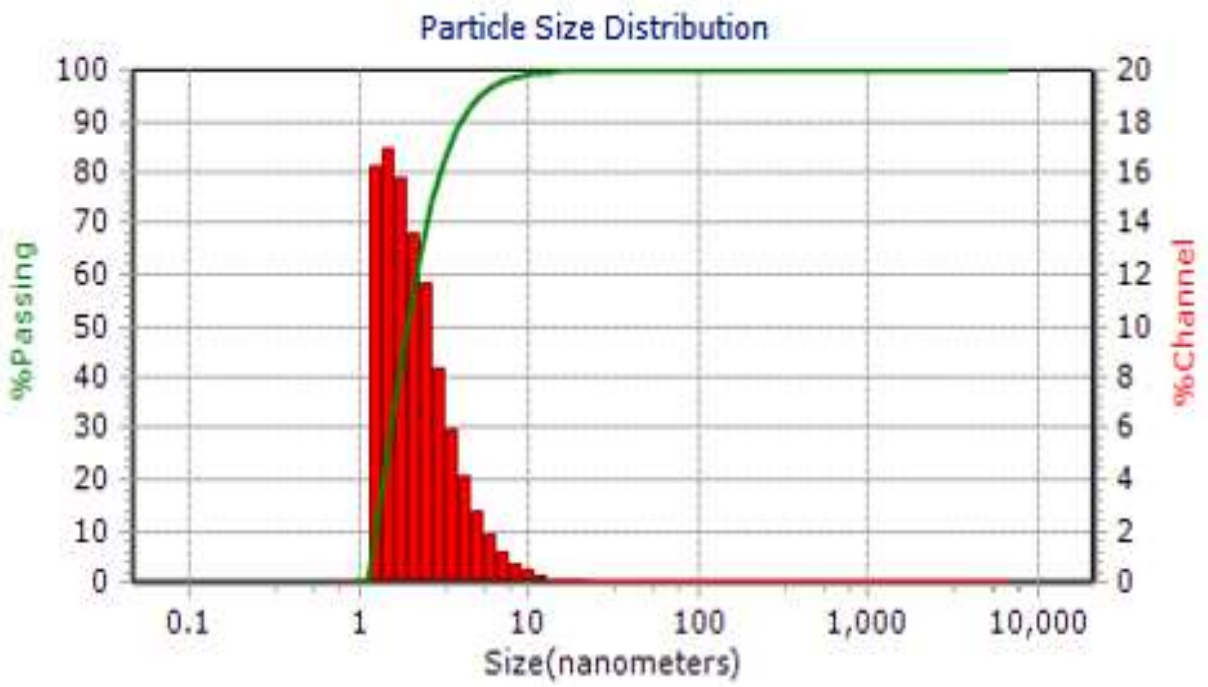

Figure 18. DLS graph for sample at 10 min reaction time dialyzed in ultra-pure water.

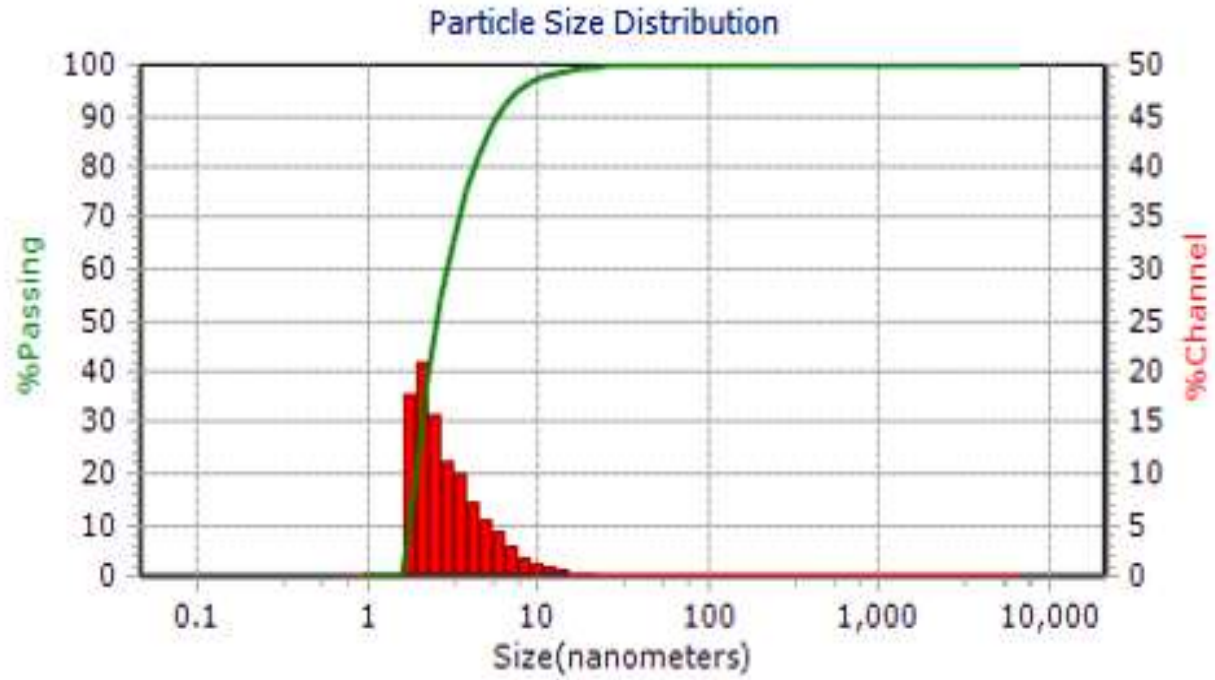

Figure 19. DLS graph for sample at 240 min reaction time dialyzed in ultra-pure water.

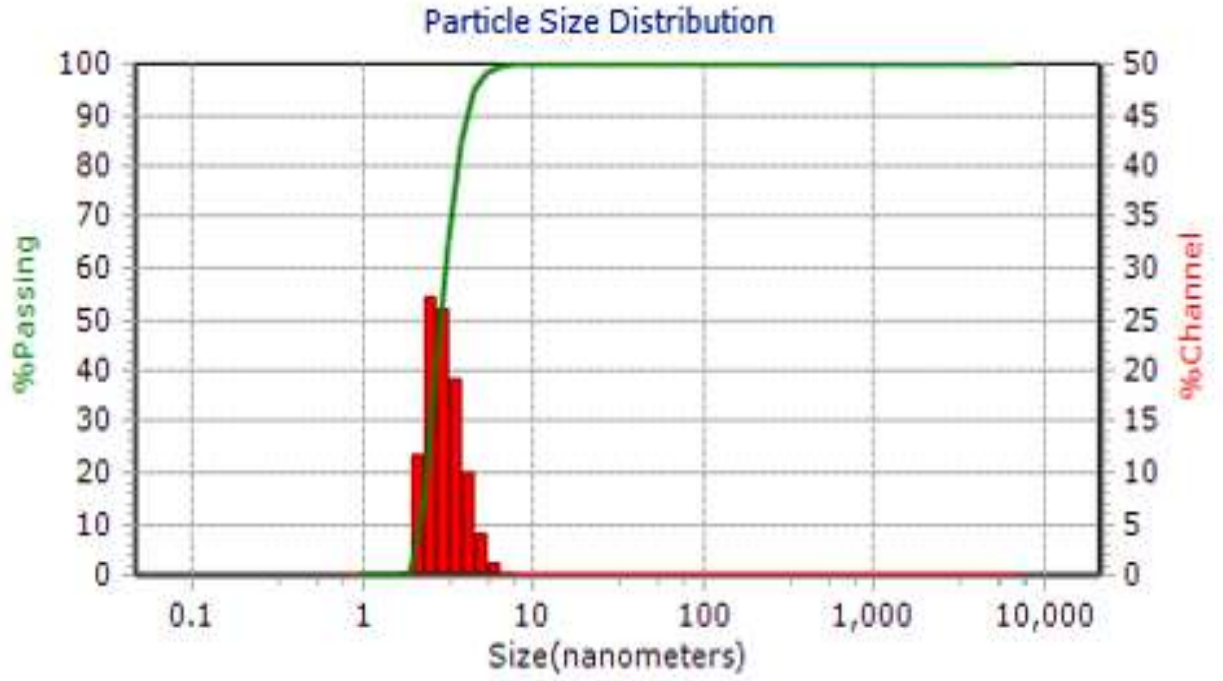

Figure 20. DLS graph for sample of protein only dialyzed in ultra-pure water.

4c) Effects of pH Using an Ultra-Pure Water as The Bulk Phase

DLS results indicated that significant aggregation could be occurring when the reaction is carried out at pH 9. While both experiments mirrored the change in the shape of the distribution noted above compared to the protein only control, the size distribution for the sample run at pH 9 extends much further past 10 nm in size. The mean size was 7.76 nm; however, the 95% confidence interval extends all the way out to 31 nm (see Table 9). This sample exhibited the greatest extent of aggregation when compared to all samples analyzed. Protein aggregation will be the subject of future studies (see Figures 21-22).

Table 9. The DLS data for varying pH.

Samples with different pH	Mean diameter of nanoparticle (nm)	Standard Deviation	Polydispersity Index	10% (nm)	95% (nm)
pH8	4.21	1.790	0.2586	2.060	9.83
pH9	7.76	3.87	0.1431	5.91	31.00

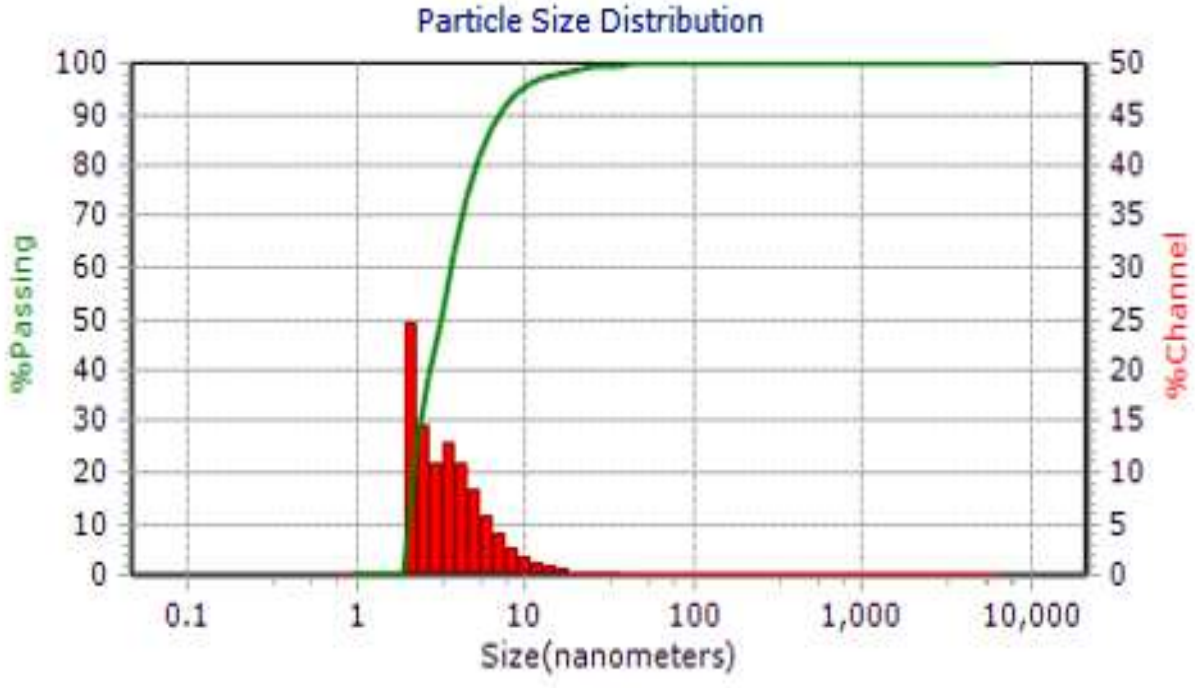

Figure 21. DLS graph for sample at pH 8 dialyzed in ultra-pure water.

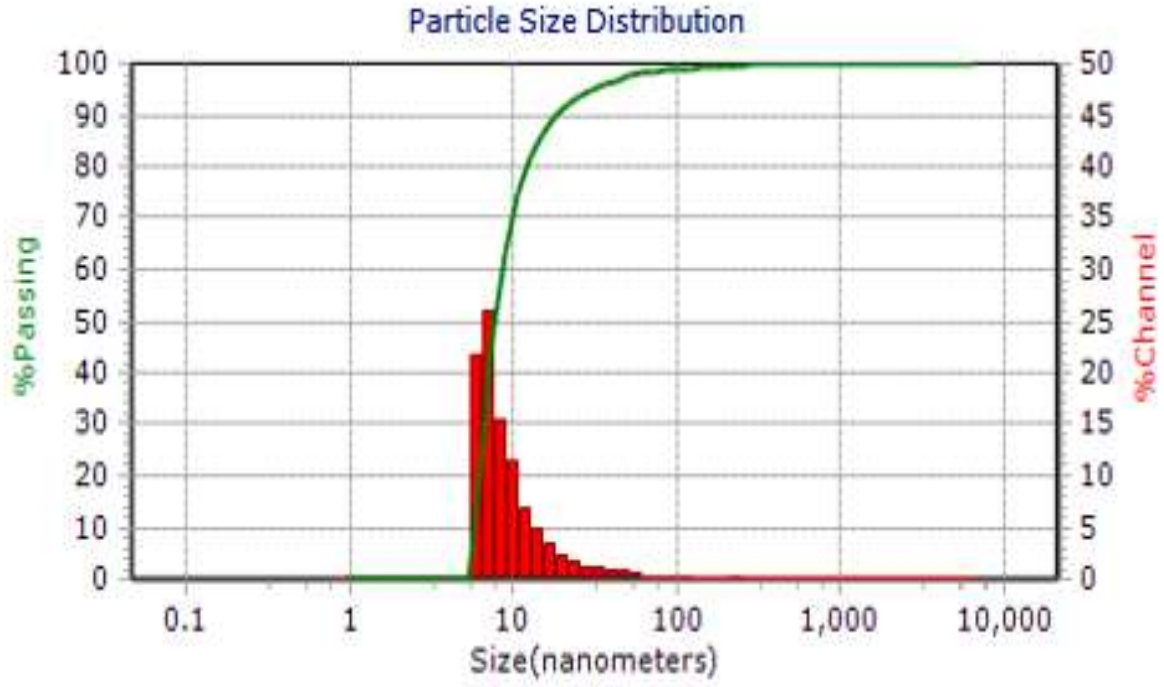

Figure 22. DLS graph for sample at pH 9 dialyzed in ultra-pure water.

5) DSC Evaluation.

Two samples from effect of reaction time using ultra-pure water as the bulk phase were used for thermal denaturation and stability studies of the protein vs conjugate. The samples used were sample 3, which contained protein only inside the cassette, and sample 1 where the reaction time was 10 minutes. The thermogram scans were collected with a range of temperature from 25 °C to 115 °C. The rate of heating for both samples was 1 °C per min, and the protein concentration was 4.4 mg/mL. The pressure was maintained at 3.0 (atm) to avoid degassing of the solutions while heating. Before analyzing the protein solutions, a baseline was obtained using bulk phase from dialysis for each sample. The reference and sample cell were first cleaned by running 200 mL of 2% micro 90 solution. The cells were than rinsed with 200 mL of ultra-pure water. All solutions were degassed at 400 atm for 15 min before injecting them into the cells. The thermograms were obtained and the T_M was evaluated using the gaussian curve. The T_M for protein was found to be

at 68.28 °C and the T_M for the conjugate was found to be at 68.00 °C (see Figures 23-24). The almost identical T_M values indicate that the tertiary structure of the protein was not degraded during the reaction. Furthermore, the stability of the protein has not been enhanced or diminished after the conjugation, which bodes well for future in vitro experiments where the tertiary structure of the protein will be key for ligand receptor binding.

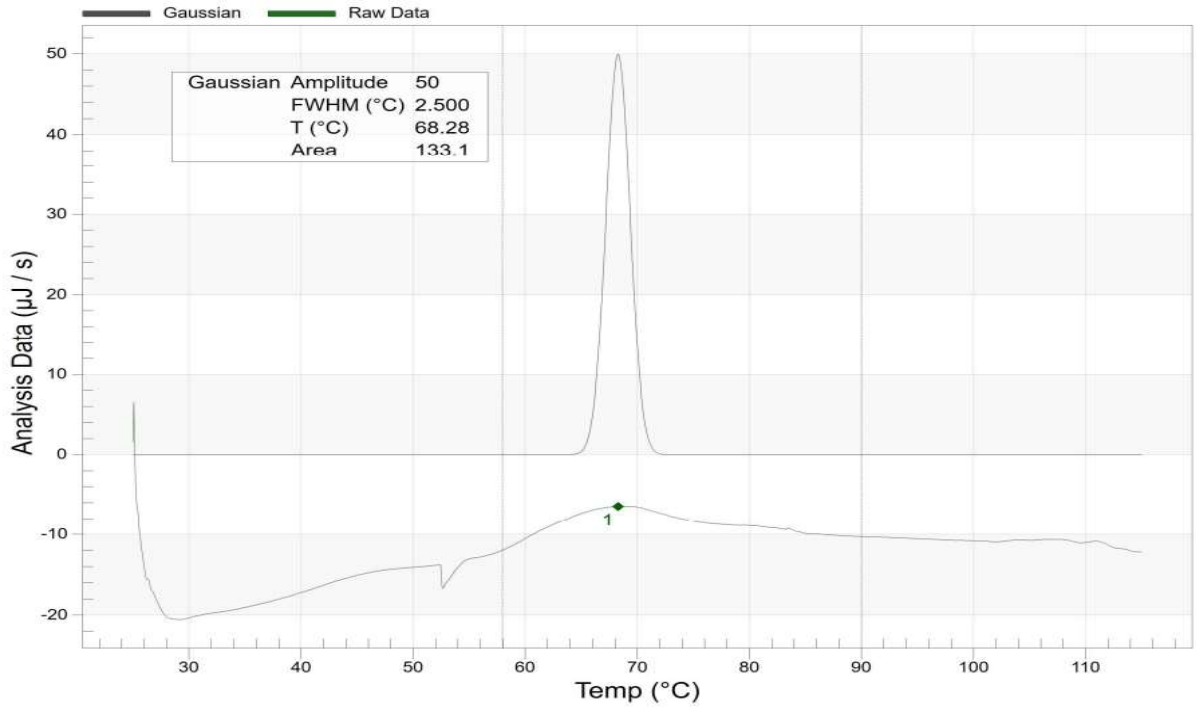

Figure 23. Thermogram for the sample containing only protein.

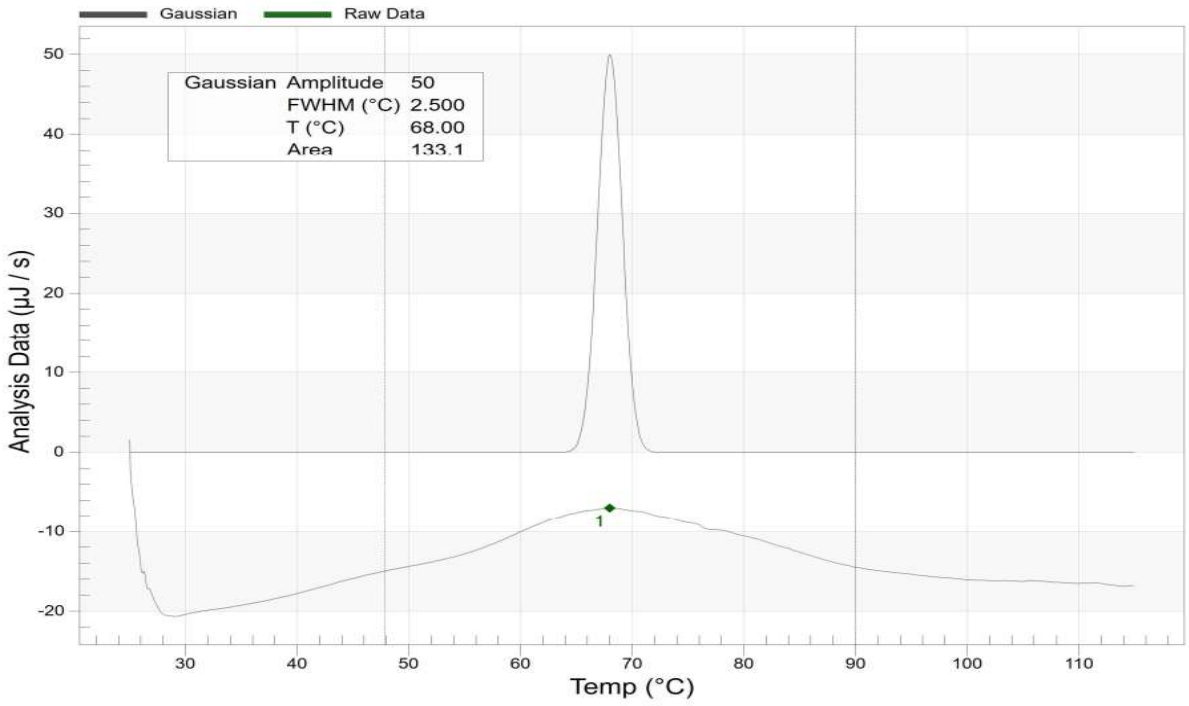

Figure 24. Thermogram for sample containing conjugate with a reaction time of 10 min and dialyzed in ultra-pure water.

CHAPTER IV

CLOSING STATEMENTS

Obtaining my bachelor's and master's degrees at Texas Woman's University was a wonderful experience. The thesis track has taught me to think outside of the box and has made me an independent scientist. My confidence working in a laboratory environment has significantly increased, will benefit me tremendously as I transition to industry. This experience has taught me how the physical, biological, and chemical concepts go hand in hand and to keep my mind open to all possible scientific outcomes when working on any scientific topic. I have learned a lot about cancer, possible treatments, and of future tools to treat cancer. Cancer is one of the worst disorders one can ever consider. The disease makes people think what they could never have expected. I do know the cruelty of cancer, but I can tell that the treatments for it are advancing rapidly.

Sometimes, we forget how far we have come in achieving something but thinking of this that I will be graduating soon, I do feel proud to have completed my master's degree in chemistry from a well-known university in the United States. I hope to use and what I have learned to help benefit society in a constructive way.

REFERENCES

1. World Health Organization. Cancer. https://www.who.int/news-room/fact-sheets/detail/cancer (accessed March 03, 2021).

2. American Cancer Society. Early History of Cancer. https://www.cancer.org/cancer/cancer-basics/history-of-cancer/what-is-cancer.html (accessed March 03, 2021)

3. Mandal, A. Cancer History. https://www.news-medical.net/health/Cancer-History.aspx (accessed March 03, 2021).

4. Gonzalez, H.; Hagerling, C.; Werb, Z. Roles of the Immune System in Cancer: From Tumor Initiation to Metastatic Progression. *Genes Dev.* **2018**, *32*, 1267-1284.

5. Manzoor, A.; Lindner, L.; Landon, C.; Park, J.; Simnick, A.; Her, M.; Shiva Das; Hanna, G.; Park, W.; Chilkoti, A.; Koning, G.; Hagen, T.; Needham, D.; Dewhirst, M. Overcoming Limitations in Nanoparticle Drug Delivery: Triggered, Intravascular Release to Improve Drug Penetration into Tumors. *Cancer Res. (Chicago, Ill.)* **2012**, *72*, 5566-5575.

6. Odularu, A. T. Metal Nanoparticles: Thermal Decomposition, Biomedicinal Applications to Cancer Treatment, and Future Perspectives. *Bioinorg. Chem. Appl.* **2018**, *2018*, 9354708-6.

7. Pang, B.; de Jong, J.; Qiao, X.; Wessels, L. F. A.; Neefjes, J. Chemical Profiling of the Genome with Anti-Cancer Drugs Defines Target Specificities. *Nat. chem. Biol.* **2015**, *11*, 472-480.

8. Barry, J.; Vertegel, A. Nanomaterials for Protein-Mediated Therapy and Delivery. *Nano Life.* **2013**, *3*, 1343001.

9. Jatzkewitz, H. An Ein Kolloidales Blutplasma-Ersatzmittel (Polyvinylpyrrolidone) Gebundenes Peptamin (glycyl-l-leucyl-mezcalin) Als Neuartige Depotform Fur Biologisch

Aktive Primare Amine (mezcalin). *Zeitschrift Fur Naturforschung Part B-Chemie Biochemie Biophysik Biologie Und Verwandten Gebiete* **1955**, *10*, 27-31.

10. Jatzkewitz, H. Incorporation of Physiologically-Active Substances into a Colloidal Blood Plasma Substitute. I. Incorporation of Mescaline Peptide into Polyvinylpyrrolidone. *Hoppe-seyler's Zeitschrift fur Physiologische Chemie* **1953**, *297(3-6*), 149-156.
11. Bangham, A. D.; Horne, R. W. Negative Staining of Phospholipids and their Structural Modification by Surface-Active Agents as Observed in the Electron Microscope. *J. Mol. Biol.* **1964**, *8*, 660-668.
12. Bangham, A. D.; Standish, M. M.; Watkins, J. C. Diffusion of Univalent Ions Across the Lamellae of Swollen Phospholipids. *J. Mol. Biol.* **1965**, *13*, 238-252.
13. Scheffel, U.; Rhodes, B. A.; Natarajan, T. K.; Wagner, H. N., Jr Albumin Microspheres for Study of the Reticuloendothelial System. *The J. Nucl. Med. (1978)* **1972**, *13*, 498-503.
14. Gradishar, W. J.; Tjulandin, S.; Davidson, N.; Shaw, H.; Desai, N.; Bhar, P.; Hawkins, M.; O'Shaughnessy, J. Phase III Trial of Nanoparticle Albumin-Bound Paclitaxel Compared with Polyethylated Castor Oil–Based Paclitaxel in Women with Breast Cancer. *J.Clin. Oncol.* **2005***, 23*, 7794-7803.
15. Cassinelli, G. The Roots of Modern Oncology: From Discovery of New Antitumor Anthracyclines to their Clinical Use. *Tumori* **2016**, *102*, 226-235.
16. Doxorubicin (Adriamycin, Rubex) Chemotherapy Drug Information. https://chemocare.com/chemotherapy/drug-info/doxorubicin.aspx (accessed January 27, 2021).

17. Papavramidou, N.; Papavramidis, T.; Demetriou, T. Ancient Greek and Greco–Roman Methods in Modern Surgical Treatment of Cancer. *Ann. Surg. Oncol.* **2010**, *17*, 665-667.

18. Jabłońska-Trypuć, A.; Świderski, G.; Krętowski, R.; Lewandowski, W. Newly Synthesized Doxorubicin Complexes with Selected Metals—Synthesis, Structure and Anti-Breast Cancer Activity. *Molecules (Basel, Switzerland)* **2017**, *22*, 1106.

19. PubChem. Compound Summary for CID 31703, Doxorubicin. https://pubchem.ncbi.nlm.nih.gov/compound/Doxorubicin (accessed January 20, 2021).

20. Cotton, S. Cobalt Chloride, A Drug Used to Dope Racehorses That's Also a Water Indicator. http://www.chm.bris.ac.uk/motm/cobalt-chloride/cobalt-chlorideh.htm (accessed February 03, 2022).

21. Zhou, Q.; Zhang, L.; Wu, H. Nanomaterials for Cancer Therapies. *Nanotechnology reviews (Berlin)* **2017**, *6*, 473-496.

22. Nguyen, D. T.; Cavazos, R. J.; Harris, A. N.; Petros, R. A. Werner Complexes Viewed Anew: Utilizing Cobalt Coordination Chemistry for 'Traceless' Stimuli-Responsive Bioconjugation Involving Therapeutic Nanoparticles, Protein PEGylation, and Drug-(Bio)polymer Conjugates. *Comments Inorg. Chem.* **2014**, *34*, 59-77.

23. Hawkins, M. J.; Soon-Shiong, P.; Desai, N. Protein Nanoparticles as Drug Carriers in Clinical Medicine. *Adv. Drug Deliv. Rev.* **2008**, *60*, 876-885.

24. Hoang, H.; Manyanga, F.; Morakinyo, M. K.; Pinkert, V.; Sarwary, F.; Fish, D. J.; Brewood, G. P.; Benight, A. S. Effects of Selective Biotinylation on the Thermodynamic Stability of Human Serum Albumin. *J. Biophys. Chem.* **2016**, *07*, 9-29.

25. Petros, R. A.; DeSimone, J. M. Strategies in the Design of Nanoparticles for Therapeutic Applications. *Nat. Rev..Drug Discov.* **2010**, *9*, 615-627.

26. Thermo Scientific™. Doxorubicin hydrochloride. https://www.fishersci.com/shop/products/doxorubicin-hydrochloride-thermo-scientific/AAJ64000MA (accessed February 03, 2022).

27. Mo, R.; Jiang, T.; DiSanto, R.; Tai, W.; Gu, Z. ATP-Triggered Anticancer Drug Delivery. *Nat. commun.* **2014**, *5*, 3364.

28. Goodman, A. M.; Neumann, O.; Kamilla Nørregaard; Henderson, L.; Mi-Ran Choi; Clare, S. E.; Halas, N. J. Near-Infrared Remotely Triggered Drug-Release Strategies for Cancer Treatment. *Proc. Natl. Acad. Sci.* **2017**, *114*, 12419-12424.

29. Gorovits, B.; Gorovits, B.; Krinos-Fiorotti, C.; Krinos-Fiorotti, C. Proposed Mechanism of Off-Target Toxicity for Antibody–Drug Conjugates Driven by Mannose Receptor Uptake. *Cancer Immunol. Immun.* **2013**, *62*, 217-223.

30. Motlagh, N. S. H.; Parvin, P.; Ghasemi, F.; Atyabi, F. Fluorescence Properties of Several Chemotherapy Drugs: Doxorubicin, Paclitaxel and Bleomycin. *Biomed. Opt. Express.* **2016**, *7*, 2400-2406.

31. Thomas Scientific. Graduated Microcentrifuge Tubes. https://www.thomassci.com/Molecular-Diagnostics/Storage/Tubes/Tubes/_/Thomas-Graduated-Microcentrifuge-Tubes?q=Plastic%20Centrifuge%20Tubes (accessed February 03, 2022).

32. Yamada, Y. Dimerization of Doxorubicin Causes Its Precipitation. *ACS omega* **2020**, *5*, 33235-33241.

33. Johnson-Arbor, k.; Dubey, R. *Doxorubicin*. StatPearls Publishing LLC, Treasure Island (FL), 2020.

34. Xue, Q.; Ren, H.; Xu, C.; Wang, G.; Ren, C.; Hao, J.; Ding, D. Nanospheres of Doxorubicin as Cross-Linkers for a Supramolecular Hydrogelation. *Scientific reports* **2015**, *5*, 8764.